REPORT DOCUMENTATION PAGE

Form Approved
OMB No. 0704-0188

1. AGENCY USE ONLY (Leave blank)

2. REPORT DATE: Aug 94

3. REPORT TYPE AND DATES COVERED

4. TITLE AND SUBTITLE
Evaluation of Calibration Parameters and Performance of the Video Imaging Technique of Assessing Exposure (VITAE system)

5. FUNDING NUMBERS

6. AUTHOR(S)
Keith M. Groth

7. PERFORMING ORGANIZATION NAME(S) AND ADDRESS(ES)
AFIT Students Attending:
University of Washington

8. PERFORMING ORGANIZATION REPORT NUMBER
AFIT/CI/CIA
94-130

9. SPONSORING/MONITORING AGENCY NAME(S) AND ADDRESS(ES)
DEPRTMENT OF THE AIR FORCE
AFIT/CI
2950 P STREET
WRIGHT-PATTERSON AFB OH 45433-7765

10. SPONSORING/MONITORING AGENCY REPORT NUMBER

11. SUPPLEMENTARY NOTES

12a. DISTRIBUTION/AVAILABILITY STATEMENT
Approved for Public Release IAW 190-1
Distribution Unlimited
MICHAEL M. BRICKER, SMSgt, USAF
Chief Administration

12b. DISTRIBUTION CODE

13. ABSTRACT (Maximum 200 words)

14. SUBJECT TERMS

15. NUMBER OF PAGES
116

16. PRICE CODE

17. SECURITY CLASSIFICATION OF REPORT	18. SECURITY CLASSIFICATION OF THIS PAGE	19. SECURITY CLASSIFICATION OF ABSTRACT	20. LIMITATION OF ABSTRACT

Evaluation of Calibration Parameters and Performance of the Video Imaging Technique of Assessing Exposure (VITAE System)

by

Keith M. Groth

A thesis submitted in partial fulfillment
of the requirements for the degree of

Master of Science

University of Washington

1994

Approved by Richard Fenske
(Chairperson of Supervisory Committee)

Michael Yost

Michael S. Morgan

Program Authorized
to Offer Degree Public Health and Community Medicine

Date August 16, 1994

Master's Thesis

In presenting this thesis in partial fulfillment of the requirements for a Master's degree at the University of Washington, I agree that the Library shall make its copies freely available for inspection. I further agree that extensive copying of this thesis is allowable only for scholarly purposes, consistent with "fair use" as prescribed in the U.S. Copyright Law. Any other reproduction for any purposes or by any means shall not be allowed without my written permission.

Signature Keith M Martin

Date 16 August 1994

TABLE OF CONTENTS

LIST OF FIGURES

LIST OF TABLES

TABLE OF CONTENTS

LIST OF FIGURES

LIST OF TABLES

CHAPTER I

INTRODUCTION

1.1 *Need for the Capability to Assess Occupational Dermal Exposure*

Assessing exposures to chemicals that can be absorbed through the skin presents the industrial hygienist with a perplexing and sometimes frustrating dilemma. The fact that three of the articles appearing in the February 1993 AIHA Journal addressed surface wipe sampling is a testament to an increasing concern over the impact of dermally absorbed chemicals. In addition to increased awareness of percutaneous absorption as a potentially major factor in total body burden, this concern probably is fueled by frequent reductions in the allowable levels of many airborne contaminants for the workplace. As allowable workplace levels drop, the percentage of total body burden that is a result of dermal absorption may increase. This is especially true if dermal exposures are not controlled as rigorously as inhalation exposures. In fact, in many instances where the chemical has a low vapor pressure and is not aerosolized, dermal absorption is the primary route of exposure (McArthur, 1992).

Although percutaneous absorption of workplace chemicals has been recognized as a very real problem, methods for evaluating these exposures are still in their infancy. In a recent OSHA rule governing the use of a suspected carcinogen that is dermally absorbed (4,4'-methylene-dianiline), OSHA conceded that in certain situations 95% of exposure comes from dermal absorption. However, OSHA failed to establish a dermal exposure limit, citing difficulties in quantifying exposures, correlating amount absorbed with risk, and inability to select a reliable biological indicator as reasons why such a limit is currently infeasible (OSHA,

1992). If an organization with the resources of OSHA, is unable to determine an appropriate method of monitoring dermal exposures to a chemical such as MDA, an independent industrial hygienists attempting to do so is faced with a daunting task.

1.2 *Current Methods for Assessing Dermal Exposures*

Currently, the sampling methods that are available to assess dermal exposures include surrogate skin, surface contamination, skin contamination, and biological. Each of these methods have inherent limitations. Used in combinations of two or more, they may be employed to sufficiently assess dermal exposures. But in some instances, as noted in OSHA's MDA rule, these methods will fall short of reliably quantifying dermal exposures. A newer technique, Video Imaging Technique for Assessing Exposures (VITAE) has been suggested as another alternative for dermal exposure assessment (Fenske, 1984). Given that current techniques are not developed enough to provide OSHA with a means of directly assessing and regulating exposures to MDA, a recognized dermal exposure problem, the introduction of another technique could be seen as a confounder in an already confused issue. Actually, this is an opportune time to explore options. Except for patch sampling to assess pesticide exposures, there are no institutionalized methods of assessing industrial, dermal exposures. Considering as many options as possible may prevent institutionalizing assessment techniques that do not optimally quantify exposures. Comparing the benefits and limitations of current methods and those of VITAE, VITAE (if validated) presents a tool to fill in many of the gaps left by current methods.

1.3 *Overview of the VITAE Approach*

VITAE is based on the principle that some chemicals fluoresce (emit visible light) when subjected to ultra-violet light. Some industrial chemicals, particularly some aromatic compounds fluoresce naturally (Fenske et al., 1986a). However, an industrial chemical that does not do so may be evaluated using VITAE by adding a tracer to the product at a known ratio to the chemical of interest. It is the presence of fluorescing compounds (tracer or target chemical) on skin surfaces that provide a marker that allows for the quantification of exposure.

After a worker has performed tasks in the workplace, body or clothing surfaces can be subjected to ultra-violet light and a video image taken. Fluorescent material on the surfaces will appear as bright areas on the image. By comparing the postexposure image with a preexposure image of the same surface, the amount of contaminant is determined by the change in total brightness of the image.

VITAE offers certain advantages over conventional approaches. First, VITAE is quick and noninvasive. It does not require application of solvents to the skin or hydration of the skin, as in handwash sampling, that might increase absorption (Bird, 1981). There is no need for laboratory analysis (after initial correlations are established) and VITAE does not require estimates of removal efficiencies. Additionally, the actual sample is retained as a permanent digital record and can be updated as analytical methods improve. Multiple samples taken throughout the day can be compared to baseline values to help pinpoint exposure episodes. Finally, the results provide a very graphic image that can be used as an invaluable

training tool for worker education.

For smaller operations, significant capital cost, not necessary for conventional methods, is required. However, in most processes that require ongoing monitoring of dermal exposures, the initial investment will probably be quickly offset by the costs laboratory analysis.

1.4 *Statement of Problem*

Although VITAE may be used without a tracer, if the contaminant of interest fluoresces strongly enough at the right wavelengths, in most cases a fluorescent tracer will be introduced to act as surrogate for the compound of interest. The amount of tracer necessary will vary, depending on the contaminant for which the tracer is a surrogate. For contaminants where it is necessary to measure very low surface densities (low target levels), relatively large amounts of tracer must be introduced. In some pesticide applications, a ratio of contaminant to tracer of as high as 5.7:1 has been used (Fenske, 1988). In other applications, where the presence of "inert" ingredients like the fluorescent tracers may dramatically impact the process or product, levels of tracer will need to be kept much lower. In fact, whether VITAE can be deemed a viable option will depend greatly on the amount of fluorescent tracer that can be introduced without degradation of the process and whether this amount of tracer is sufficient to be reliably measured by the imaging system. On the other hand, too much tracer can create problems for VITAE, regardless of whether or not it impacts the product or process. If the intensity of the light emitted by a high density of tracer on any portion of the skin exceeds the maximum level that the imaging system records, these high intensities will be recorded as intensity levels near the top of the dynamic range of the

imaging systems. Consequently, these greater than quantifiable intensities will be falsely recorded as lower levels and the method will underestimate the true exposure. Additionally, quenching may take place at higher surface densities of tracer that will result in unacceptable correlation between predicted and actual surface densities of tracer (Fenske et al., 1986b). Finally, use of the VITAE method by Black (1993) as part of an overall assessment of children's exposure to Chlorpyrifos from activity in treated lawns also revealed that variability of subjects' natural florescence (background brightness) can affect the intensity of florescence emitted by the tracer. Pervious work using VITAE sought to correct for background gray level by using a standard curve developed by exposing marked areas of skin with known amounts of tracer and developing a relationship between the background gray level and the irradiance of the tracer at different concentrations (Fenske et al., 1990; Black ,1993). However, the effectiveness of this method has not been determined, nor has it been determined whether using this approach of correcting for background gray level significantly impacts the outcome.

As these considerations indicate, an investigator wishing to use VITAE for dermal exposure assessment must introduce fluorescent tracer in amounts that fall within what can be termed an "operational window". The lower bound of this window is determined by the desired target surface density of the contaminant, the maximum amount of tracer that can be added without degrading the process, and the amount of fluorescent tracer that must be used to achieve surface densities of tracer that can be reliably quantified. The upper bound of the window is dictated by the upper quantifiable limit for the method. It becomes apparent that the investigator must know both the lower and the upper quantification limits for the VITAE

system before it can be determined if the introduction of an appropriate amount of tracer is feasible. These values will be impacted by several factors, including, masking of fluorescence from other materials present on the skin, interference from other fluorescing compounds, and variability in individual skin characteristics.

The preceding discussion presents several issues that must be addressed if VITAE is to be a valid tool for assessing occupational, dermal exposures. First, it must be demonstrated VITAE predictions correlate well to know tracer densities. Second, it must be shown that the impact of varying skin pigmentation (background grey level) can be controlled across the quantifiable range of the system. Third, a lower quantifiable limit must be established and exposures exceeding this limit reliably identified by the system. Finally, it must be show that an upper quantifiable limit can be determined, allowing investigators to calculate the maximum concentration of tracer that can be introduced and still produce acceptable correlations to contaminant concentration.

CHAPTER II

STUDY DESIGN

2.1 *Introduction*

A two phase approach was used to address the issues outlined in the preceding chapter. First, a summary standard curve was developed, using a wide range of skin pigmentations and doses so that the system is calibrated to handle a variety of conditions. From the images used for the summary curve, the parameters used to construct the curve and the assumptions made in using them were tested. How well the calibration data was described by the summary curve was evaluated by determining the tracer densities of the calibration images using the VITAE system and the known tracer surface densities. The second phase of the study was designed to test the method under simulated exposure conditions. Images were taken after applying two different exposure distributions to the hands of volunteers. The performance of the system when the distribution of surface contaminant was different from the distribution of the calibration exposures was evaluated using these images.

2.2 *Background of Summary Standard Curve*

As noted earlier, a summary standard curve that relates median background grey levels to tracer irradiance at different tracer densities has been used to adjust for the effects of background grey level. Variability of skin between individuals is, to say the least, complex. The amount of body hair, relative oil content of the skin, and skin imperfections like scars,

acne, or callouses are but a few of the myriad of factors that might impact the degree to which a tracer fluoresces. Attempting to identify, quantify, and correct for all variables would be too unwieldy. However, one gross measure of skin variability, background grey level (BGL), has been noted by previous investigators to noticeably impact the light emitting characteristics of fluorescent tracers (Fenske, et al., 1990; Black, 1993). The BGL of a skin surface may be determined by more than just the degree of skin pigmentation. Oil and water content, as well as body hair and other factors may influence the natural irradiance of the skin. Therefore, adjusting images based on a gross, descriptor like background grey level may actually incorporate the effects of other more specific factors.

The standard curve is, in effect, a model of relationships between natural background brightness, tracer surface density, and the change in brightness due to the addition of the tracer. None of the previous literature discusses the assumptions upon which the model is constructed or attempts to assess the performance of the method when the tracer surface distributions are different from those of the calibration method. To accomplish this, the modelling process must be detailed and the assumptions inherent in the model must be identified.

2.3 *Outline of Summary Curve Construction and Application*

The summary curve is constructed by using images of marked skin areas of human subjects. Images of the subjects are taken before and after varying, known amounts of tracer are applied in a consistent manner to the marked areas of skin (the process is detailed fully in the Methods chapter). Using VITAE software (Fenske, 1991) three histograms are produced; a preexposure, a postexposure, and a net histogram.

The preexposure and postexposure histograms provide the number of pixels at each of the 256 grey levels (0 - 255). From these histograms the median and average grey levels of the image and image brightness are determined. The brightness is simply the integrated area of the histogram.

A net histogram is generated by the VITAE software. It is produced by subtracting the number of pixels at each grey level in the preexposure histogram from those of the postexposure histogram and setting any negative values to zero. This means that the net histogram is not a true integrated difference between the postexposure and the preexposure histograms.

To develop the summary curve the median grey level of the pixels that represent exposed skin is needed. The postexposure histogram is a combination of two distributions; one of pixels that represents skin exposed to tracer and one of pixels that represents unexposed skin. Because of this, the median of the postexposure histogram is not an appropriate estimator of central tendency. Previous VITAE work used calibration images with high exposures and their net histograms to determine the number of pixels exposed to tracer in a calibration image (Fenske, 1990; Black 1993). Images of high tracer surface densities yield postexposure histograms where the distributions of the exposed and unexposed pixels are distinct. The net histogram, for these cases, were assumed to represent the pixels that correspond to exposed areas of skin. The median grey level of the net histogram for these images can be used for the summary curve because in this case the exposed pixel distribution can be separated from the unexposed pixels. All cases of bimodal postexposure histograms were identified and average number of pixels in the net histograms was

determined. Since the tracer was applied in a consistent manner to the same size area for all exposures, this average number of pixels was considered the number of exposed pixels and was used to determine the median grey level of exposed pixels for images where the two distributions of the post exposure histogram were not distinctly bimodal. This was done by using postexposure histogram. Starting at the highest grey level, the number of pixels for each grey level were incrementally added to a cumulative sum of pixels. The median grey level of the exposed pixels for distributions without distinct modes was assigned to the grey level whose contribution to the sum, made the cumulative sum equal to or greater than half the average number of pixels from the net histograms of the high surface density images. This grey level is referred to as the calibration grey level.

Images are then grouped according to their median BGL. Response curves are developed for each group of background grey levels (e.g. a single response curve might be developed for background grey levels 21 thru 23). The group response curves are linear regressions of the natural logarithm of calibration grey level of exposed pixels versus the logarithm of tracer skin loading (pg/pixel). The slope and intercepts of these BGL specific group response curves are then both regressed against the natural logarithm of the average of the median BGLs of each group. The resulting summary curve is actually two curves that describe a family of curves. The summary curve provides the slope and intercept of a linear curve that predicts how the BGL of a skin surface will impact the fluorescence of the tracer.

The VITAE software uses the summary curve information and the net histogram from image pairs of exposed subjects to predict the amount of tracer present on a skin surface. It does this grey level by grey level, applying the equation from the summary curve to each grey

level of the net histogram and then multiplying the result by the number of pixels in the grey level. This provides an estimation of the amount of tracer represented by each grey level. The sum of these provides an estimate of the total tracer present.

2.4 *Evaluation of the Model's Mathematical Relationships*

As discussed previously, the summary curve process is actually a method of modelling several imaging variables. If one considers a single pixel of an image from a tracer exposed skin surface, the brightness of the pixel will depend on the inherent brightness of the skin (background), the brightness due to the tracer loading, and a term that describes the interaction between the background and the tracer loading. This can be described conceptually in equation form as:

$$\ln Pixel\ \ Brightness = a * \ln Background + b * \ln Tracer + c * f(\ln Background\ ,\ \ln Tracer\ ) \qquad \text{(Eq. 2.1)}$$

Where

a, b, and c are constants.

The current summary curve method uses the median grey level of the preexposure histogram to describe the tracer surface density associated with each grey level in the net histogram. The description of the tracer density for a given net histogram grey level can be considered in equation form as given by:

$$\ln Mass\ /pixel = (C_1 \ln BGL + C_2)\ln Exposed + C_3 \ln BGL + C_4$$

(Eq. 2.2)

Where

C_1 = Slope of Slope Summary Curve
C_2 = Intercept of Slope Summary Curve
C_3 = Slope of Intercept Summary Curve
C_4 = Intercept of Intercept Summary Curve
Exposed = Individual Net Histogram Grey Level
BGL = Median Grey Level of the Preexpsoure Histogram

Equation 2.2 was derived from the empirical, graphic methods outlined by Black (1993). Although the VITAE calculating program uses several steps, it applies the same information in an equivalent manner to each grey level of the net histogram. This indicates that the surface density and the brightness are logarithmically related. Besides being supported by the empirical data, this is the recognized relationship between the optical density and brightness (Russ, 1992). However, the loading rate is not the dependent variable and the equation might be more appropriately written:

$$\ln Exposed = \frac{\ln Mass\ /pixel - C_3 \ln BGL - C_4}{C_1 \ln BGL + C_2}$$

(Eq. 2.3)

Equation 2.3 differs from Equation 2.1 and introduces several issues that may affect the performance of the system. First, as opposed to Equation 2.1, this equation is nonlinear (when using log transformed data). Also, there is no discrete term for the brightness that is due to the tracer density. Additionally, there is a peculiarity that exist due to the nature of the

equation. The equation breaks down when the average BGL is less than one. In fact, regardless of the surface density or the grey level of the histogram being evaluated, the calculated density approaches infinity as the average BGL approaches zero. This condition exists because the calibration method generates a negative number for C_3. Since the grey level scale does not encompass absolute dark or bright, this may be a governing condition when the pigmentation of the imaged surface is very dark.

2.5 *Identification of System Parameters and Assumptions*

The VITAE uses the summary curve to describe how a specific element of skin, represented by a pixel, will fluoresce given the BGL of the skin element and the amount of tracer present on the surface. This interaction is modelled by exposing an area of skin several thousand times greater than the area represented by a pixel to a known density and measuring certain parameters that describe the distribution of pixels before and after exposure.

2.5.1 Describing Distributions Using Measures of Central Tendency

The summary curve method uses measures of central tendency to describe the distribution of pixels in the preexposure and net histograms. For the preexposure histogram, the method uses the median grey level. The calibration grey level described in Section 2.3 is used to describe the distribution of pixels that represent skin surface that is exposed to tracer. These exposed pixels are represented by the net histogram. The reason the median of the net histogram is not used is due to the way the method was developed. The calibration grey level predates the inclusion of the net histogram in the VITAE calculation program.

If these measures of central tendency describe the distribution well, they will be strongly correlated to the integrated brightness of their corresponding histogram. This was

tested by performing linear regressions of the central tendency parameters and their corresponding integrated brightness. In addition to a strong correlation, the intercept of the regression line should be zero. This hypothesis was also tested.

2.5.2 Symmetry of Distributions

The summary curve process treats calibration images as if the distribution of grey levels are uniform (all pixels have the same grey value). The preexposure images are assigned a single grey level (the median) and the exposed pixels of the postexposure image are treated as if the tracer density and resulting grey level are uniform when the response is related to the tracer density. Since the video ramp is linear, uniform distribution is not essential, but symmetry is. If the distribution is symmetrical, the pixels brighter than the central grey level will balance out the pixels darker than the grey level.

The output of the VITAE calculation program does not provide data that lends itself to any rigorous testing of symmetry for the histograms. However, if a linear regression of the median and the mean of the histograms yields a slope that is not significantly different than one, then the assumption of symmetry would not be unreasonable. In addition to this, the histograms were also visually inspected for obvious asymmetry.

2.5.3 Independence of Samples

Although it has not been addressed in any of the previously published literature that employs or evaluates the VITAE system, there are several assumptions about the independence of samples that are inherent in the summary construction. The construction of the summary curve requires that the images be grouped according to their BGL, but irrespective of either their anatomical location or the subject from which they were acquired.

This requires that the VITAE method be independent of these factors.

Fenske et al. (1990) noted that the response of the system did not appear to be subject or anatomical location dependent. However, these observations have not been supported with statistical testing. These assumptions of independence were tested by developing a response curve of the system using the same images that were used for the summary curve construction. If the response of the system is independent of both the subject and the anatomical location, so will the residuals of the response curve. These conditions were tested using the response curve described in the following subsection and analysis of covariance for the effects of anatomical location and subject.

2.6 *System Response Curve*

The predicted loading of the VITAE method can be considered an adjusted response of the system. It measures the response of the system and corrects for the effects of BGL. If the grey level range covered the spectrum of grey levels from absolute black to infinite brightness and if there was no electronic noise associated with the system, the response (i.e. the relationship between predicted and actual loadings) would be linear. However such is not the case.

The VITAE system is, in effect, a photon counter. The charge-coupled device (CCD) camera, imaging board, and filters employed in the system actually screen and count the photons that are associated with the irradiance of a surface of interest. The lower limit of the tracer density that can be reliably detected by this system is determined by several factors. First is the effects of electronic noise. In addition to the effects of temperature and power fluctuations on the performance of the more than 245,000 sensors that are associated with an

image, there is the simple fact that this many sensors cannot be manufactured to respond identically to the same input of photons. These factors create electronic noise in the system that, when photon flux is low, can be statistically important (Russ, 1992). The second factor that influences the density of tracer that can be detected by the system is the amount of tracer that is necessary to create enough change in brightness to cause a pixel in the image to raise at least one grey level. As noted earlier, this quantum requirement is dependent on the BGL. But there is a level at which all BGL will reveal a response. The third factor is experimental variability. Actual doses and areas are calculated from measured values and as such suffer from inherent variability. These factors are impossible to completely separate and determine the amount of tracer than can be detected above both the electronic noise, the quantum density requirements, and experimental variability. Together, they can be termed system noise and determine the extent of the low, flat portion of the theoretical response curve shown in Figure 2.1, as well as the transition to the linear portion of the curve. Surface densities were left in the log transformation since the system models the data to fit a linear curve in this form and evaluation of the models performance should be done in the same form.

The upper, flat portion of the curve, as well as the transition from the linear portion of the curve (Figure 2.1) is also influenced by several factors. The first, is suppression of tracer irradiance due to the effects quenching. The phenomena was noted by both Black (1993) and Fenske et al. (1990) and results from either tracer densities that are high enough to block UV radiation from reaching some of the tracer molecules and/or the presence of enough tracer that a significant portion of the tracer does not receive enough energy to fluoresce. The second factor is simple saturation of the detectors. The imaging board only

records grey levels to 255. Light intensities (photon flux) that would result in grey levels higher than 255, given the existing linear ramp, would be recorded as 255 (Rich et al., 1989).

As the system response gets higher, the contribution of system noise to the signal becomes less significant and the response curve should be related to irradiance of the imaged surface. This relationship should remain until quenching and detector saturation are significant contributions to the signal. If the images of the calibration doses are well described by the summary curve model, this portion of the curve, where neither electronic noise, quenching, nor detector saturation contribute significantly to the response, should lend itself to linear approximation. This model of system response, graphically portrayed in Figure 2.1, provides a way of testing how well the summary curve approach models the effects of loading and BGL, determining the operating range of the system, and testing the assumptions of sample independence outlined in the preceding subsection.

2.7 *Assumptions of Summary Standard Curve Application*

Another assumption of uniformity/symmetry is necessary for the VITAE program to apply the standard curve to net histograms. When the VITAE calculating program estimates the amount of tracer that corresponds to a given grey level in the net histogram, it treats the pixels in that grey level as if their distribution were uniform or symmetrical and as if their distribution were the same as the distribution of pixels in the preexposure histogram. This may not be true if features on the skin that tend to have abnormal grey levels (e.g. hair, scars, callouses, skin creases) also tend to either collect or avoid tracer differently than the

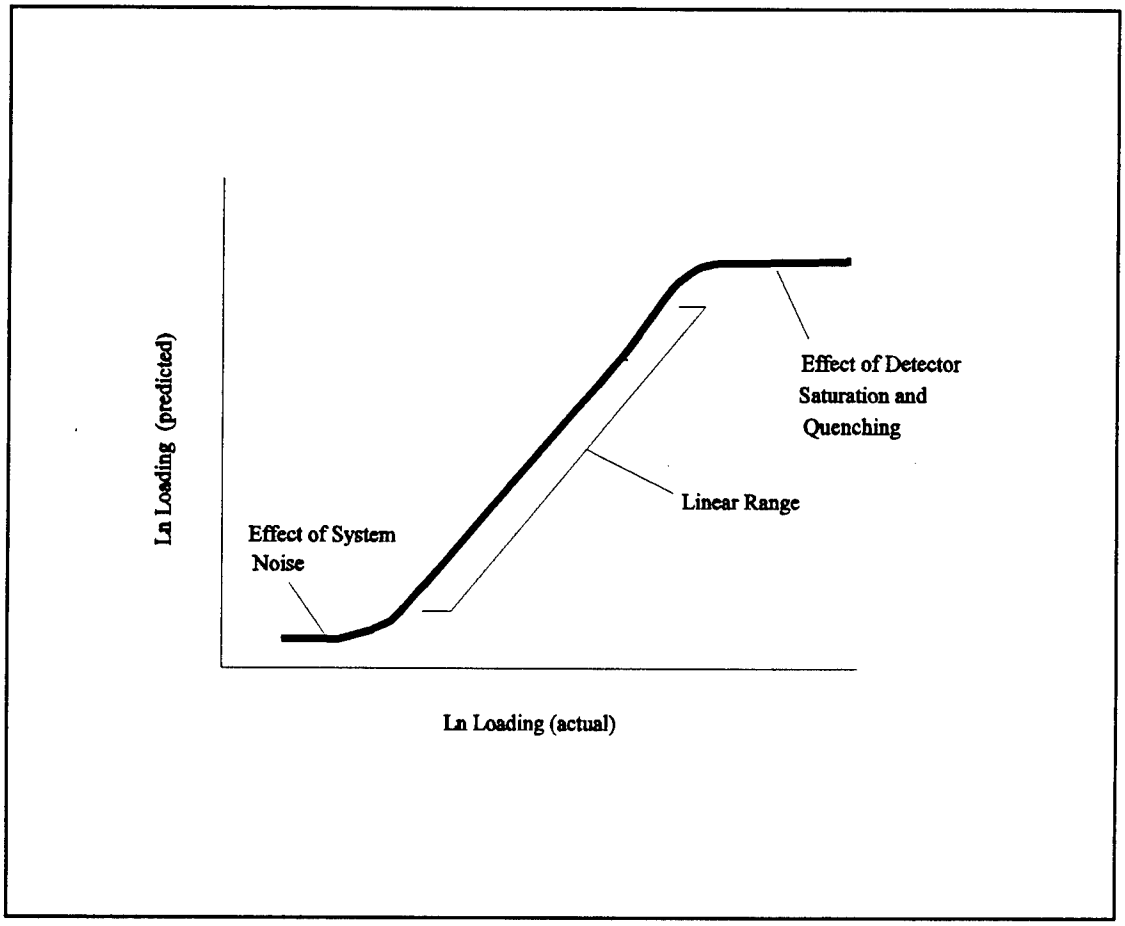

Figure 2.1. Theoretical Response Curve

remainder of the surface. Unfortunately, testing this assumption of symmetry is not feasible, given the imaging technology employed in the method.

The VITAE system uses the median BGL to construct the summary curve, but uses the mean BGL when it applies the summary curve data to each of the net histogram grey levels. This has the advantage of avoiding logarithms of zero for dark images with median BGL of zero. However , it demands that the two parameters do not differ significantly. If this is true, then the same test used to test the symmetry of the preexposure histogram will validate this assumption.

Probably the most critical assumptions that are associated with the summary curve application is the assumption of performance. If the summary curve is based on valid assumptions and relationships then it will correct properly for the BGL and the relative accuracy will not be dependent on the loading (density). This was tested using the regression of the *ln* loading (predicted) vs the *ln* Loading (actual). The residuals of the doses that fall along the linear portion of the curve were tested to establish that it was reasonable to assume their distribution was normal. These data were grouped according to dose (this will make the densities nearly equal). Analysis of variance was then performed to test the assumption that the model properly corrects for grey level. If the assumption is valid, then a significant portion of the variance of the residuals would not be described by the BGL. The performance of the system in predicting loading was tested in two parts. The first was to perform another analysis of variance, using the dose groups, to determine if a significant portion of the residual variance was described by the loading. The second part was to test the slope and intercept of the response curve for significant difference from an identity function. If the VITAE system predicts the loading perfectly, then the slope of the curve will be unity (one) and the intercept will be zero. These parameters were tested for the regression.

2.8 *Operating Range of Summary Standard Curve*

As with any analytical instrument, the operating range of the system must be determined to have a practical application. Black (1993) used changes in distribution to decide whether an image represented an exposed surface. This is a feature offered in the VITAE calculating program. The program detects changes on integrated brightness between the preexposure and the postexposure images and/or shifts in the maximum grey level. The

amount of change required to identify a surface as exposed is determined subjectively by the investigator. This approach has several drawbacks. First, the relative change in brightness is dependent on BGL. Therefore, a surface density identified by the criteria as exposed for one subject may be deemed unexposed for another subject. Secondly, the criteria have not been tested for any set of values and known exposures. A more straightforward approach was used for this study. The detection limit was calculated for the linear portion of the response curve. If the assumption of normality of residuals is correct and if the loading does not significantly contribute to residual variability, then the variance among dose groups should be relatively equal. Given this, the residuals can be pooled and the 95% confidence interval of the untransformed loading is given by:

$$95\%\ CI = e^{\ln Loading - 1.96 \cdot StdDev} ; e^{\ln Loading + 1.96 \cdot StdDev} \qquad \text{(Eq. 2.4)}$$

Where

StdDev = the standard deviation of the pooled response curve residuals

Equation 2.4 is not the 95% confidence interval of the line that describes the response curve. Rather, it is a confidence interval of the response of the system for any given loading (within the linear range of the model). Ideally, if the confidence interval can be expressed as a function of the true value, then setting the lower bound of the confidence interval equal to zero and solving for the corresponding loading would give the detection limit of the method. However, the model is based on equal variance across the linear range of the response curve and the response curve is a logarithm relationship. This implies that the variance of the

untransformed data approaches zero as the loading approaches zero. This may be more readily seen if the equation for the lower bound is rewritten as:

$$95\%\ CI,\ Lower\ Bound\ = \frac{e^{\ln Loading}}{e^{1.96 \cdot StdDev}}$$

(Eq. 2.5)

However, in this case the model also provides a practical solution. If the assumptions discussed earlier are met, the slope of both the model response curve and the curve of the untransformed data will be unity. Given this, the detection limit can be determined using the distance of the lower bound from the untransformed response curve. When this distance is equal to the loading, there will be greater than 95% confidence that these readings are associated with actual tracer response and not system noise. The detection limit then is given simply by:

$$Detection\ \ Limit\ = e^{1.96\ \cdot\ StdDev}$$

(Eq. 2.6)

Equation 2.6 is the detection limit of the system and not the lower limit of quantification. The lower limit of quantification is also determined by the loading at which the response curve can be described as a linear relationship. This only becomes and issue if the detection limit falls below the lower end of the linear range.

As with the lower limit of quantification, the upper limit is driven by the linear portion of the response curve. The upper limit of detection will be determined using both the

assumption of unity for the response curve and the 95% confidence interval. If the addition of the samples from a dose cause a significant shift in the response curve from unity or if the average response of the dose falls outside the 95% confidence interval, the next lowest dose will be considered the upper limit of quantification for the method.

2.9 *Simulated Exposures*

Thus far attention has been focused on the summary curves, mainly determining if the assumptions inherent in their development and application are valid, how well the method models the calibration exposures, and what will be the range of the method. Even if the assumption are reasonable and the model describes the calibration data well, a critical question remains. Will the VITAE system respond comparably when the exposure conditions are not as constrained as the calibration exposures? In other words, it must be shown that the system response is not dependent on the distribution of the tracer on the skin. A practical way of testing this is to simulate exposures that might be expected in an occupational exposure, using known amounts of tracer.

Simulated exposures were done using the hands of volunteers. The hands were chosen for several reasons. They provide a convenient area to image, are easy to manipulate and do not require the removal of clothing. They also present rather complex surfaces, so they provide a good challenge for the system. Two exposure patterns were used, one involving the palm of the hand and the other using the dorsal portion of the hand. Palm doses were developed to simulate exposures that workers might receive when gripping contaminated surfaces. The exposures to the dorsal portion of the hand simulated deposition of droplets as might occur during spraying of pesticides or paints. Both exposures were

performed so that the amount of tracer deposited on the skin was known.

Images were analyzed using the VITAE system and the summary standard curve data. Response curves were constructed for both exposures by regressing the logarithm of the VITAE estimates of densities against the logarithm of the known tracer densities. The assumption that the system response is independent of distribution was tested by examining the parameters for the regressions of the two simulated exposures. If the assumption is valid, the regressed lines will not differ significantly from the response curve of the calibration images. That is, their slopes and intercepts will not differ significantly from the regression line associated with the calibration images.

2.10 *Dose Ranges*

Early work by Fenske (1986a) noted a detection limit of about 100 ng/cm^2, the beginnings of quenching effects at 700 ng/cm^2, and an upper quantifiable limit of about 2000 ng/cm^2. These limits were estimated from a gross examination of a standard curve produced using various tracer densities. The curve was developed without correcting for the effects of background grey level on tracer irradiance. Additionally, the study a used different camera, imaging board, and tracer. Black (1993), on the other hand, used the same equipment and tracer employed in this study. She noted a loss of linearity in the grey level response curves below a dosing concentration of 8 ppm and above 800 ppm. These limits translate to skin densities of approximately 12.5 ng/cm^2 and 1250 ng/cm^2. She provides no explanation on how it was determined linearity was lost or if an attempt was made to model the relationship between tracer density and irradiance outside these ranges.

Using the Turner 430 Spectrofluorometer, the lowest dose that can be reliably

administered to the palm of the hand is about 0.4 ng/cm^2. Dosing for the development of the standard curve and both simulated exposures thus began at this level encompassed a range that yielded surface densities of at least 1250 ng/ cm^2.

CHAPTER III

METHODS

3.1 *Equipment and Materials*

3.1.1 Tracer

A fluorescent whitening agent (FWA) with the trade name Uvitex OB (2,2'-(2,5-Thiophene-diyl)-bis (5-tert-butylbenzoxazole) (Cas 7128-64-5)) was used as the tracer in this study. Uvitex OB was chosen as the tracer for the following reasons:

1. It does not exhibit significant toxicity (Review of toxicological data is provided in Appendix A).

2. The emitted fluorescence of Uvitex OB is fairly stable over time and under exposure to UV energy (Lee, 1990).

3. Has adequate retention by the skin (solubility in water 0.01 g/100 mL).

4. Is readily soluble in acetone and toluene (0.5 and 5.3 g/100 mL respectively) to allow for dosing solution and proper elution from glass surfaces.

5. Uvitex OB has distinct and well separated extinction (375 nm) and fluorescence emission (435 nm) peaks.

3.1.2 Imaging Hardware

A. Camera:

All images were acquired using a Cohu 4810 monochrome Charge-coupled device (CCD). The camera collects 754 x 488 pixels.

B. Lens:

A Fujinon TV Zoom Lens - H6x12.5R was used for all image acquisition. The lens has eight principal f/stops (f/1.2 -f/16) and zooms from 12.5 to 75 mm.

C. Lens Filter:

A Kodak No. 2E Wratten Gelatin Filter was used to filter light entering the lens. The filter was secured to the lens end with a 52 mm technical filter holder. The filter blocks wavelengths below 410 nm, while transmitting light of longer wavelengths (~ 75%). This filter reduces interference from reflected UV and white light, but allows detection of fluorescence emitted by the Uvitex OB (435 nm).

D. Illumination:

Image surfaces were illuminated by two banks of four 4 foot F40 BLB (blacklight bulbs). The blacklights emit energy from 330 to 415 nm with the peak at 355 nm. The lights do not emit middle or short wave. Each bank of blacklights was filtered by selective glass filters developed by Fenske (1984). These filters further restrict the wavelengths illuminating the imaged surfaces, eliminating wavelengths above 400 nm.

E. Imaging Board:

Analog to digital and digital to analog conversions were accomplished with a Data Translation 2851 High Resolution Frame Grabber. The imaging board supported image capture (frame grabbing), image restoration, and computations. The imaging board provided a resolution of 512 x 480 pixels. This allows for the capture of less pixels (in both dimensions) than the camera senses. The excess pixels (upper rows and right columns) are

simply truncated with only the captured pixels appearing on the monitor screen. The imaging board assigns each pixel a numerical value to indicate relative brightness based on a 0 to 255 grey level scale. The scale, or video ramp is linear.

F. Computer:

Imaging software was run on an IBM-compatible computer (Dell 486P/33) with a 120 MB hard drive and 8 megabytes of RAM. Image manipulation (outlining and setting reference points) was performed using a Logitech three button mouse. Due to the memory intensive nature of image processing and limited hard drive space, images not being processed were stored on a 60 megabyte tape drive (Mountain Filesafe Tape Drive Series 7060).

G. Monitor:

Images were viewed for manipulation and examination using a Sony Trinitron Color Video Monitor (model PVM-1342Q).

3.1.3 Software

The software used to capture, display, and manipulate images, outline images, examine individual pixels, and provide pixel distribution data (histograms) was originally developed by Dr. William Gibb and was revised by Dr. Kyugon Cho. They are a collection of individual programs written in Microsoft C and utilizing software written specifically for the Data Translation video boards.

3.1.4 Analysis of Tracer Solutions

All tracer solutions were analyzed using a Turner 430 spectrofluorometer. Tracer was analyzed in solutions of toluene. The excitation wavelength of the spectrofluorometer was set at 355nm and the emissions were measured at 450nm.

3.2 *Subject Selection*

This study was unfunded. As such funds were limited and compensation of subjects to participate in the study was not available. Because of this, subjects were recruited from the students of the University of Washington's Environmental Health Program and their friends. Efforts were made to include as much ethnic diversity as possible, so that the full range of background grey levels and brightness that might be encountered in field evaluations would be included in this study. For the same reason, both males and females were included as test subjects. All subjects were briefed on the potential hazards of participation and the aims of the study. Consent forms were competed for each subject. A copy of the consent form is included as Appendix B.

3.3 *Imaging Technique*

The same imaging technique was used for both standard curve images and simulated exposure image sessions. There were differences in dose application, positioning of imaged surfaces, and image outlining in the two session types. Details for each are outlined in their corresponding sections later in this chapter. Following is a step by step overview of the imaging technique:

A. Setup:

The equipment was setup in a light tight room. The walls around the equipment were covered with darkroom curtains. The equipment was not moved during the study.

1. Camera: The camera was set level on a tripod with the lens center 100 cm above the floor. The f-stop was set on at 1.2 for all images. The focal length was set at 20 mm and the camera focused on the subject frame. Both the zoom and the focal rings were taped to

prevent movement when the lens was capped/uncapped or the f-stop was adjusted.

2. Subject Frame: The subject frame (constructed of 1 in by 2 in pine and painted flat black) was situated on a metal stand 125 cm from the detector of the camera. Its center was in line with the camera line of aim and 100 cm above the floor.

3. Lights: Each light bank was set on a stand with the center of the tubes oriented floor to ceiling and with their centers 100 cm above the floor. Both light banks were pointed toward the subject frame with the filter surfaces parallel to the subject frame. The distance between the light bank and subject frame planes was 90 cm. The centers of the banks were separated by 100 cm, making each center 50 cm for the camera line of aim.

The stands for the subject frame and light banks were connected at their bases to prevent inadvertent movement. Figure 3.1 provides a schematic view of the equipment layout.

B. Warm-up:

Prior to any imaging, lights and camera were allowed to warm up for at least one hour to allow the light emissions and camera system noise to stabilize.

C. Black Image:

Prior to all imaging sessions an image was taken with the f- stop closed and the lens cap in place. This image would be used later by the VITAE program to correct for system noise.

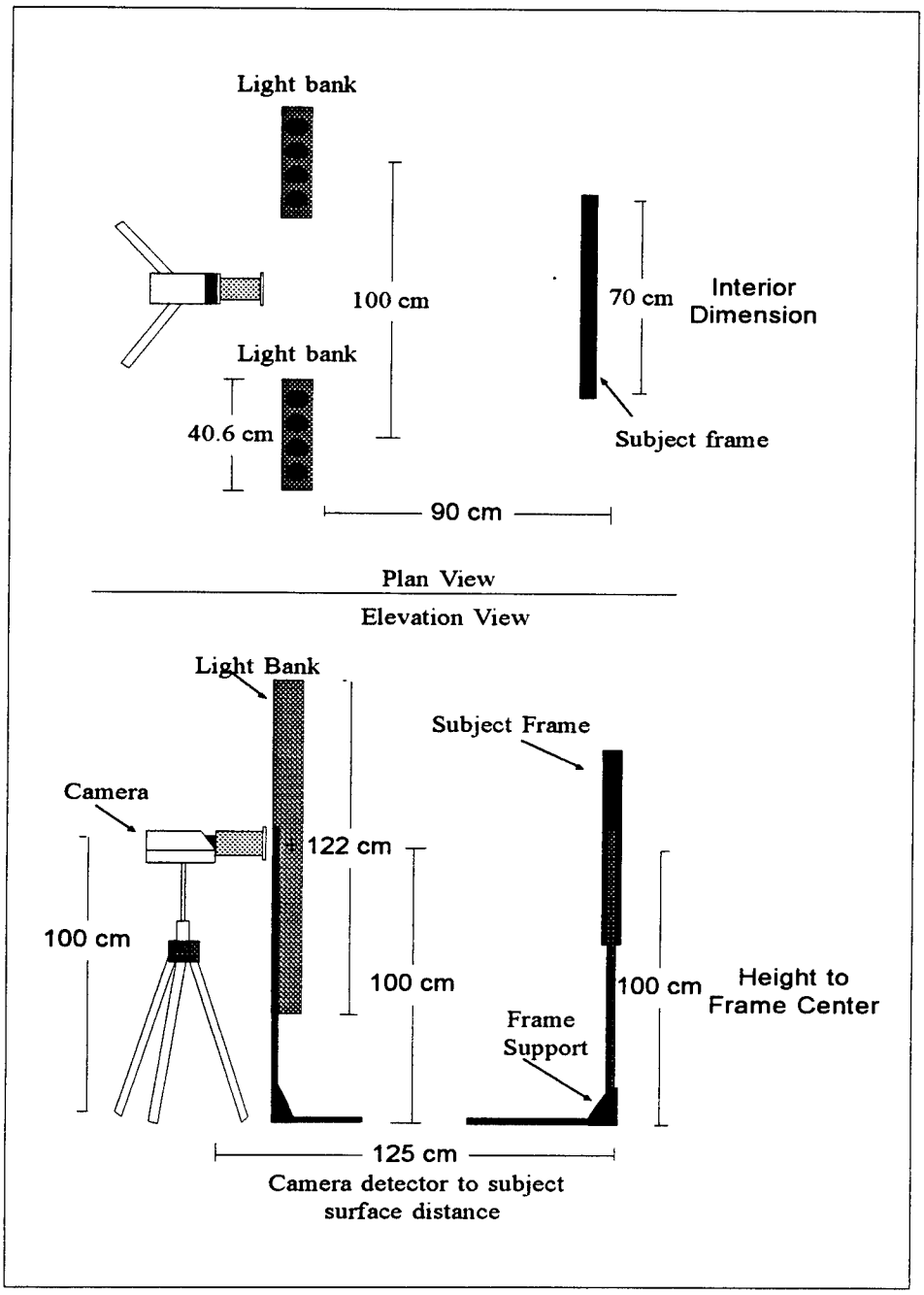

Figure 3.1. Equipment Layout

D. Standard Target - Initial:

An images of a standard target was used throughout the study to correct for fluctuations in the light energy produced by the black lights. An image of the standard target was acquired prior to the all subject imaging. Regardless of how many subjects were imaged in a day, each subject had separate standard target images. A piece of 75% cotton fiber white paper was used as the standard target. The same piece of paper was used throughout the study and care was taken to prevent soiling the target. The VITAE program prompts for initial standard target image as part of its image acquisition routine.

E. Preexposure Image:

Preexposure images were taken using the Image acquisition routine in the VITAE program. The standard body location identifiers in the program were not used, instead the "other" option was used for all image application. Awkward positions were avoided during imaging to make preexposure and postexposure images as comparable as possible.

F. Dose Application:

Doses were applied as described in the pertinent sections of the following text.

G. Postexposure Image:

Postexposure images were taken less than three minutes after preexposure images. This was done to limit the possibility of crosscontamination or loss of tracer through unintentional contact of exposed skin surfaces. Since each subject had several doses applied and were required to reposition for imaging after dose application, subjects were carefully monitored and controlled to prevent inadvertent contact of exposed areas.

H. Standard Target - Session End:

Directly after the last postexposure image of each subject a session termination standard target image was taken. The same target used for the initial standard target image was used for the termination standard target.

3.4 *Summary Standard Curve Sample Collection*

3.4.1 Preparation of Doses

Ten exposure doses were made by dissolving Uvitex OB in acetone. The concentration of the doses were chosen so that lowest doses would yield surface densities below the linear range or the detection limit and the highest dose was above the concentration where quenching begins as discussed in Section 2.10. The interval between concentrations was chosen so that the natural logarithms of the doses were evenly spaced. This was done because the summary curve is based on the logarithms of the surface densities. Additionally, this spaces the concentrations closer together at the low end of the dose range, allowing for a more accurate determination of the detection limit. The doses developed were 0.28, 0.68, 1.44, 3.72, 9.52, 20.56, 61.12, 157.6, 425.8, and 1084 mg/L. As figure 3.2 shows, these doses do follow a log-linear increase from the lowest to highest dose. The same standard doses were used throughout experiment and were stored in capped 10 mL volumetric flasks, in 4°C freezer when not in use.

3.4.2 Special Setup

The equipment was set up in the same manner as described in section 3.3, except for the addition of a special target board. This board was constructed by painting a 72 cm x 72 cm x 1/4 in. polyfoam board flat black and cutting a 5 1/2 cm square hole in the center. The

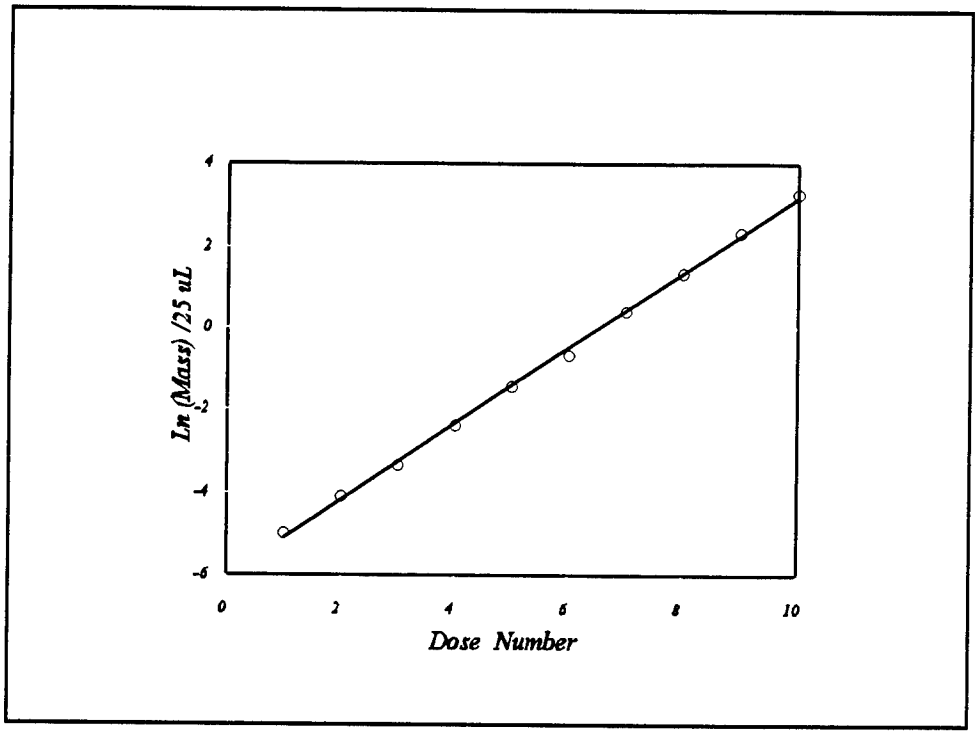

Figure 3.2. Distribution of Doses - Summary Standard Curve

board was attached to the back to the subject frame by four wing nuts, one in each corner.

3.4.3 Standard Target

The standard target image was taken by placing the target directly behind and flush to the polyfoam board.

3.4.4 Target Selection and Preparation

Targets (5 cm x 5 cm areas of subjects' skin) were marked using a 6 cm x 6 cm square of black construction paper with a concentric 5 cm x 5 cm hole cut in the center. Each interior corner was marked with a very small dab of fluorescent yellow paint. This was done to simplify the outlining process and to reduce error for any outlining where the boundary between the target marker and the subject's skin was difficult to visually distinguish. Target

markers were attached to areas of interest using a water soluble, nontoxic, pressure sensitive adhesive.

Eight areas were imaged for each subject. Areas were chosen from both the left and right palm, dorsal portion of the hand, inside of the forearm, and outside of the upper arm. Areas were chosen that presented a relatively planar surface. No surface preparation was performed on the imaged areas nor was effort taken to avoid or remove body hair.

3.4.5 Preexposure Positioning and Imaging

Preexposure images were not taken all at once but rather were taken as part of an image set. In other words, the first postexposure image was taken before the second preexposure image. Images were take by having the subject behind the polyfoam board with the marked area visible through the hole in the board. Since the hole in the target marker is slightly smaller than the hole in the polyfoam board there was some play in subject positioning. Prestudy trials revealed that making both marker and board holes the same size made it extremely difficult to ensure that the entire marked area was visible to the camera. A subject was considered properly positioned when all four fluorescent paint dots were visible on the monitor. Awkward positioning of the subject was avoided. This was generally done by having the subject find a comfortable position behind the board with the area of interest visible through the board hole and then placing the target marker in the same relative position.

3.4.6 Dose Application

Doses were applied in a controlled, random manner. Assignment of doses to each imaged area was performed prior to the imaging session. This was accomplished using a computerized random number generator, randomly assigning numbers from one to ten for

each of the eight areas. Doses for the palms and back of hands were controlled to ensure that at least two images for each dose were taken of both the back the hand and the palm. This was accomplished by rejecting an assigned dose if two images had already been acquired at the assigned dose for the controlled area (back of the hand or the palm). If a dose was rejected, another random dose was generated until it was not rejected. No distinction was made which side, right or left, had been imaged. This was done until two images at each of the ten doses were acquired for both the back and palm of the hand. Once these forty images were taken, any additional subjects imaged for the standard curve were assigned doses in an uncontrolled, random manner.

Doses were applied using a 25 uL positive displacement pipet (plunger - glass tube style). Using the pipet and 25 uL of the assigned concentration, the dose was applied by slowly depressing the plunger of the pipet while moving the tip across the marked area. Even distribution was obtained moving the pipet parallel to an edge, zigzagging back and forth down the length of the marked area and then repeating the process in a perpendicular direction. Care was taken to apply the dose about 1 cm from any marker edge and to apply the dose slowly enough that the solution would not wick outside the area of application.

For each summary curve image session four controls were taken for each dose used. Using the same pipet used for dose application, a 25 uL volume was placed in four separate sample jars. Toluene was added to each sample jar and the solution analyzed using the Turner 430 Spectrofluorometer. The mass applied for each dose was determined using these controls. This was done to ensure that no doses were contaminated during the study or that dose solutions were concentrating through evaporation from improperly sealed containers.

3.4.7 Postexposure Imaging

Postexposure images were taken as soon as the acetone was no longer visible on the surface. Since only 25 uL was used and it was spread of approximately 16 cm^2 this usually took less than a minute. The subject was positioned behind the board with the marker still in place. Again, it was ensured that all four florescent paint dabs were visible in the monitor before the image was acquired.

3.5 *Simulated Exposure Sample Collection*

3.5.1 Special Set-up

Images were acquired using the same image setup outlined in Section 3.3 except for the addition of two features to the image frame. First, a positioning line was added to the subject frame. The positioning line is made of black silk thread and was run horizontally across the image frame approximately 25 cm from the top. A small piece of marking tape (1 cm x 1 cm) was attached to the center of the positioning line to help subjects consistently position their hands. A shielding curtain was also added. The curtain, made of darkroom, cloth was hung from the top, back of the subject frame to cover the entire frame area.

3.5.2 Standard Images

For consistency, standard images for simulated exposure sessions were taken in the same manner as used for summary curve sessions. The black polyfoam board was in place, with the target paper directly behind.

3.5.3 Preexposure Image Acquisition

All images of simulated exposure were of both hands. Subjects were seated behind the picture frame with the middle finger of each hand touching the positioning line. This and the

marking tape, that was used for centering the hands in the subject frame, provided a way of consistently positioning the hands throughout the session. To ease the outlining process and to increase consistency, the hands were positioned with the fingers extended and pressed together. The subjects were asked to hold their hands so that the imaged surface was as planar as possible. The investigator ensured that the surface of interest (either the palms or the backs of the hands) were parallel to the subject frame. The shielding curtain was dropped between the hands and body of the subject so that the imaged surface was seen against a black background.

3.5.4 Dose Application

A. Palm Doses:

Doses were applied to the palm of the hands by having the subjects grip test tubes that were spiked with the tracer. Test tubes were spiked with solutions of acetone and Uvitex OB, using a 50 μL positive placement micropipettor and the same method as described in Appendix C. Twenty spiked tubes were prepared for each subject (ten for either hand). The subject gripped each tube once, starting with the lowest dose and increasing in dose. Using the data develop in Appendix D, doses were applied to the tubes so that surface densities would begin below the anticipated detection limit (linear range) and exceed the density where quenching was anticipated. Exposure images were taken after the pair of tubes at each dose were gripped. For the first eight tube pairs, subjects were asked to grip the tube firmly with one hand lift it from the peg rack and return it to the peg rack. The contact time was approximately two seconds. The subjects were asked to contact the tube with the outside blade of the hand first to prevent deposition of tracer on the area between the index finger and

the thumb. Tracer deposited here would be missed when the palm was imaged. The process was repeated using the opposite hand and the other tube of the dose pair. The last two tubes for each hand were held lightly by the subject, while being slowly spun by the investigator. This was done in an effort to achieve detector saturation for some images.

B. Dorsal Doses:

Doses were applied to the dorsal portion of the hand using a 25 μL positive displacement pipettor and solutions of acetone and Uvitex OB of varying concentrations. Each subject had six to eight doses to each hand, with the doses applied in increasing concentrations. Both the left and right hand were dosed and imaged together. Images were taken after each dose. The same dose was given to either hand at each dosing. The solution was applied by touching the pipettor to the skin surface, moving the pipettor form the surface, depressing the plunger so that a meniscus was developed extending from the end of the capillary tube, and then recontacting the surface. This was repeated until the tube was emptied and the plunger contacted the skin. The contacts were made in as random a manner as possible. To aid in this, doses were applied under white light where the tracer from previous contacts during the dosing and from previous dosing sessions would not be seen by the investigator.

3.5.5 Postexposure Image Acquisition

Postexposure images were taken as soon as the acetone on the skin had dried (about two minutes). Postexposure images were taken with the subject duplicating prexposure positioning as much as possible. Special attention was paid to ensure that the relative positions of the fingers and thumbs were constant.

3.6 *Image Pair Analysis*

3.6.1 Outlining

The VITAE system requires that the area of interest on the images be outlined. This is performed using a mouse. The program allows either straight line or freehand drawing, depending on mouse button manipulation. The postexposure image is outlined and then two reference points are chosen on the image. Next, the same two reference points were chosen on the prexposure image. From these, the program draws the outline around the prexposure image. If the fit is unsatisfactory, the reference points can be chosen again or the entire outlining process can be redone. The calibration images were outlined using the florescent paint dots. Straight lines were drawn using four points just inside the paint dots. The simulated exposures were outlined using a series of very short straight lines. This provided better control of the process. It was ensured that, whenever possible, no background (black area) was included in the outline.

3.6.2 Calculation of Tracer Mass

The VITAE system does not calculate the tracer density. It provides the mass of the tracer, which is a summation of the masses relating to each grey level. The program corrects for the effects of lens distortion, adjusting the histograms of the images before calculation of the mass associated with each grey level. On the other hand, corrections for variations in illumination are made when the total mass is calculated. The program uses ratio of the average standard target grey level to session end grey level to correct for difference in illumination between calibration and exposure measurement illuminations. The ratio of initial to session end grey levels are used to correct for variations in illumination within a session.

The VITAE program provides the mass in micrograms after the corrections have been made. The density is calculated using this, the number of pixels in the outlined area, and the pixel dimensions determined in Appendix E.

CHAPTER IV

RESULTS AND DISCUSSION

4.1 *Summary Curve Construction*

4.1.1 Subjects

A. Results:

A total of 11 subjects were recruited for the summary curve portion of the study. The subjects yielded 88 image pairs, but only 82 pairs were used in summary curve development; one image pair was lost because the investigator failed to acquire a preexposure image, two images were discarded because postexposure images showed tracer solution had wicked beyond the marker boundary, and one image was lost in data transfer. Additionally, two images were not used because the preexposure brightness was greater than the postexposure brightness. The VITAE computer code generates a positive mass in these situations because after subtracting the preexposure histogram from the postexposure histogram, it sets all negative values to zero to produce the net histogram. Therefore, the magnitude, of what should be a negative response, can not be estimated. The demographics of the subjects are given in table 4.1.

B. Discussion:

The diversity of the subjects provided a wide range of median background grey levels. The median background grey levels ranged from 0 to 51, which covers nearly one fifth of the dynamic range of the system as it was set up. This diversity in background grey levels allowed the method to be tested over a considerably greater range than was tested by

Table 4.1. Demographics of Summary Standard Curve Subjects

Race	Sex	
	Female	Male
African-American	0	1
Asian	1	1
Caucasian	2	5
Hispanic	1	0

previous investigators. Using this calibration approach, Fenske et al. (1990) covered median background grey levels from 8 to 32, Black (1993) used levels from 3 to 23, and Archibald (1994) used grey levels from 4 to 18. Although these values are not directly comparable since the grey level measured for a surface is dependent on the lighting conditions, the equipment setup, and the equipment used, the range of grey levels as a fraction of the system dynamic range is comparable. This is due to the fact that all studies used the same imaging board, making the dynamic range equivalent, and the video response to light intensity is linear for the system. Given this relatively wide range of background grey levels, this study will provide the ability to test the system performance in correcting for the effects of background grey levels on tracer irradiance.

4.1.2 Grouping Images

As indicated by Fenske et al. (1990) the standard curve images were placed into groups based on the median background grey level of the image. The groups were chosen by trying to achieve groupings with similar sample size and without having images with the same background grey level in two different groups. Specific data for the images in each group are

supplied in Appendix F, while Table 4.2 provides a summary of grouping information.

Table 4.2 Summary Standard Curve Groups, by Median BGL

Group	N	Range of Median Grey Levels	Average Median Grey Level
1	12	0 - 9	3.17
2	12	10 - 14	12.67
3	12	15 - 17	15.92
4	11	18 - 21	18.27
5	12	22 - 29	25.87
6	12	30 - 38	33.25
7	11	40 - 51	43

4.1.3 Calibration Grey Levels

Of the 82 image pairs used, 19 had postexposure histograms that were clearly bimodal, with the modes well separated. This was determined through visual inspection of individual histograms. The average number of pixels in the net histogram for these images was 2426 (CV = 10%). Calibration grey levels were determined for each image pair using the 2426 pixel value, the postexposure histograms, and counting back method described in Section 2.3 of the preceding text. The value determined for each postexposure image is included in Appendix F.

4.1.4 Effects of Extreme Values on Linearity

The VITAE method requires that the logarithm calibration grey level be regressed (linear)

against the tracer loading (calculated in pg/pixel) for each background grey level grouping. As discussed earlier, Black (1993) noted a loss of linearity in this relationship, when the loading values were extreme. Because of the small sample size of each group and the variability present, rigorous methods of deciding when the impact of extreme loading rates affect the regression was difficult. Similarly, visual inspection of scatter plots had the same problems. The approach chosen was to perform several regressions on each group, each time deleting a group(s) of image pairs associated with doses at either end of the dose range. This approach is similar to that used by Fenske et al (1990). The effect of these deletions on the regressions is provided in Appendix G. Deletion of the lowest dose and then the two lowest doses affected the slopes and intercepts of the individual grey level group curves and the summary curves as well as resulting in a consistent increase in R^2 for both the group and summary curves. Deletion of the highest dose, after the two lowest does have been deleted, does not make as dramatic an impact on the summary curve parameters and the effect on the correlation coefficients is inconsistent. For these reasons the summary curves were developed using the highest eight doses administered, but deleting the lowest two doses. The BGL-specific group response curves are presented as Figure 4.1 and the resulting summary curves are presented in Figure 4.2.

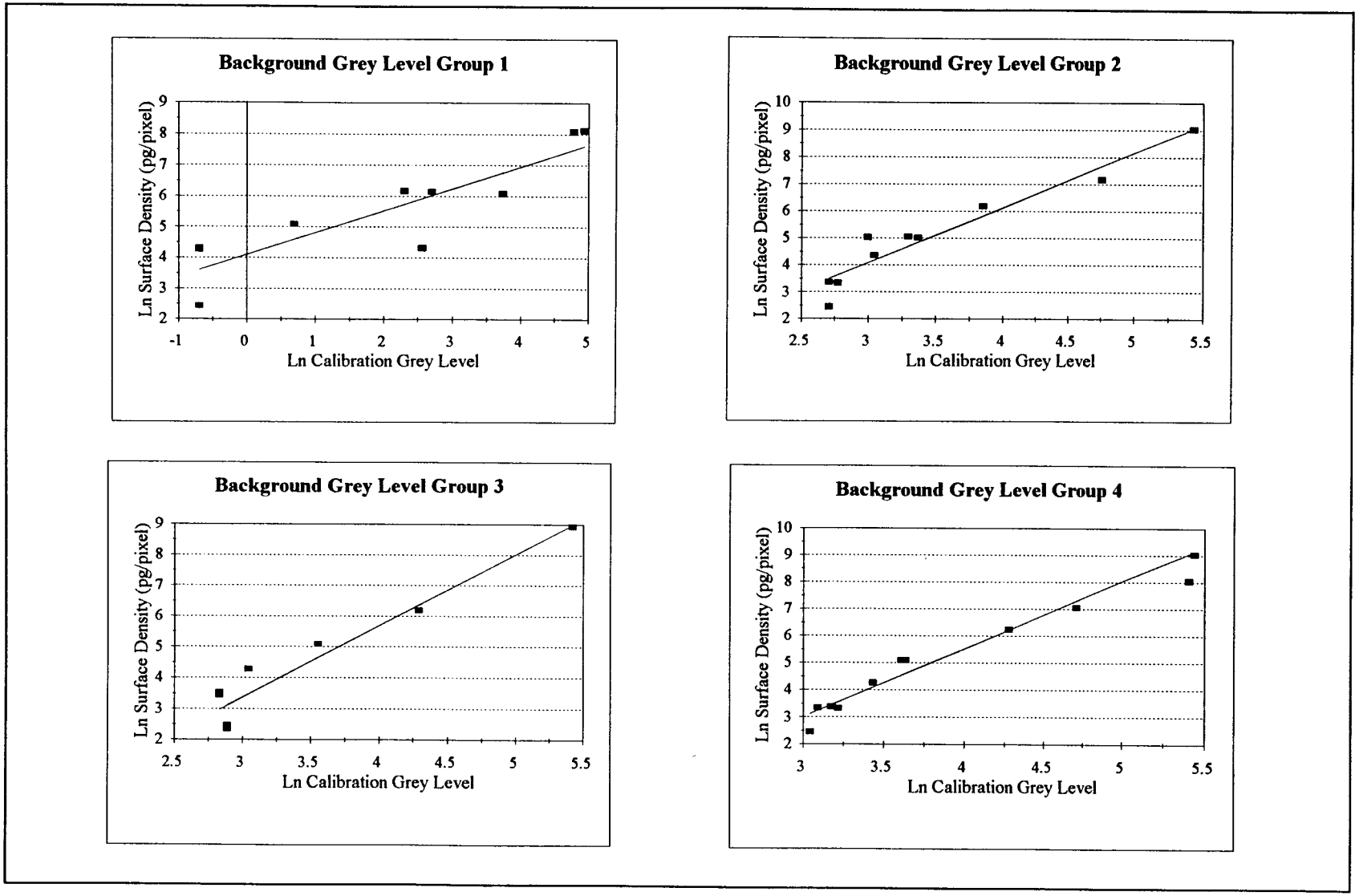

Figure 4.1 Background Grey Level Group Response Curves

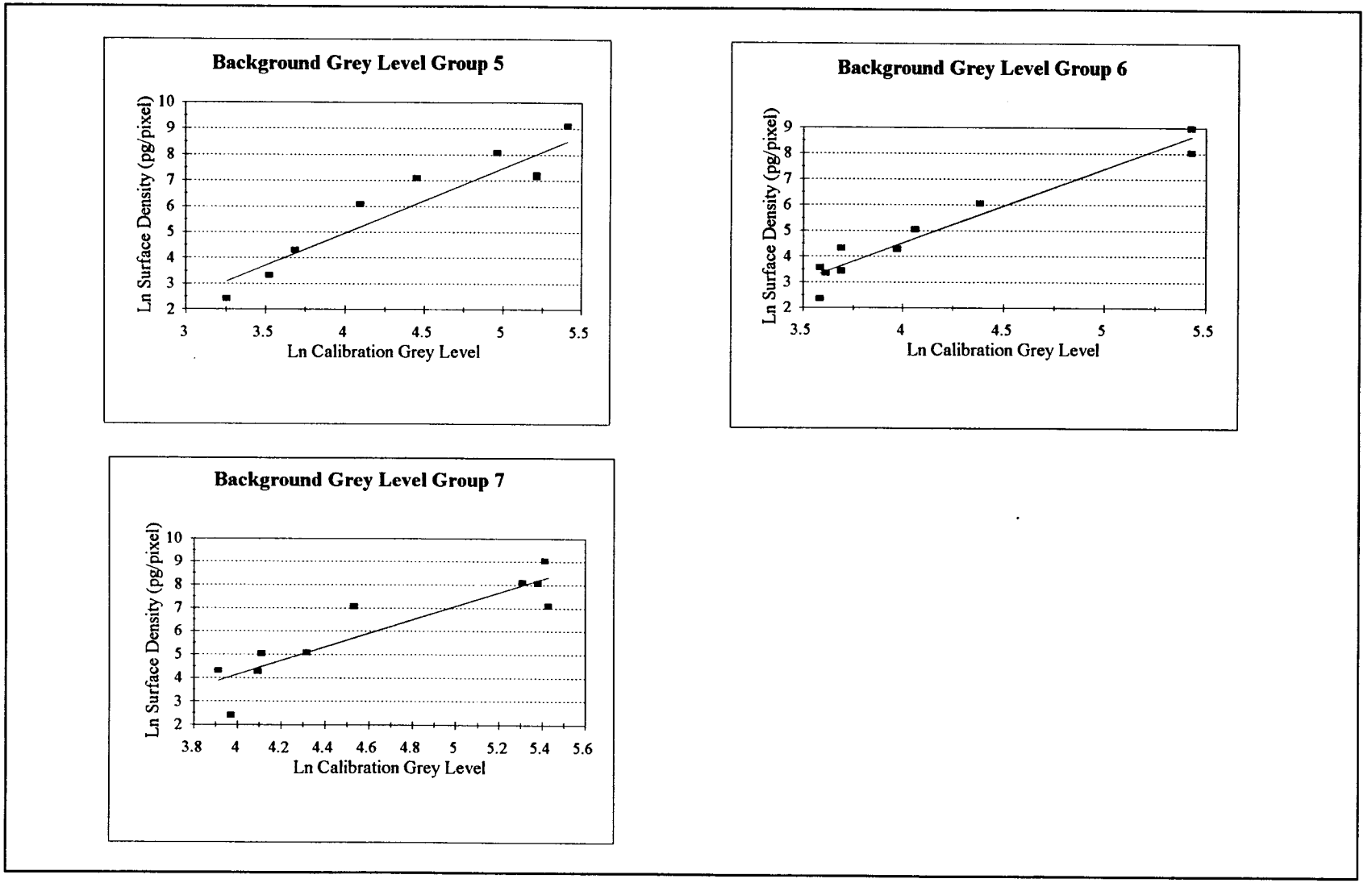

Figure 4.1 Continued

Figure 4.1 cont.

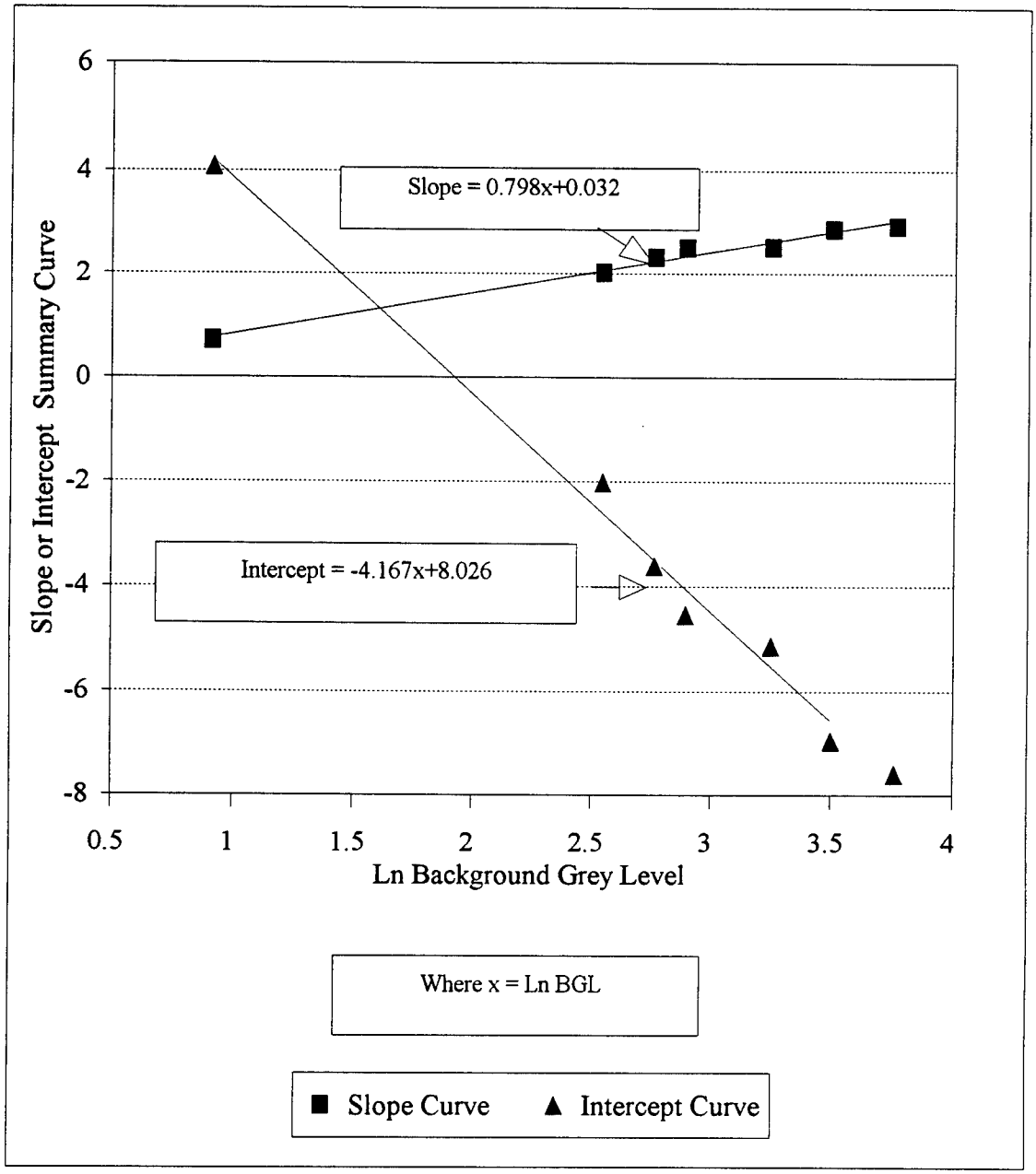

Figure 4.2. Summary Standard Curves

4.2 *Testing of Summary Standard Curve Development Assumptions*

4.2.1 Describing Distribution Using Measures of Central Tendency

As Figure 4.3 shows, the median of the preexposure histogram proved to be strongly correlated to the integrated brightness. A linear regression produced an R^2 of 0.978 and the constant (-2172) that was not significantly different than zero (p value = 0.15). The median grey level appears to be a good descriptor of the preexposure histogram.

On the other hand, the relationship between the calibration grey level and the net integrated brightness was not as good. Although the R^2 remained high (0.973), Figure 4.4 reveals this was probably due to the cluster of data points at either end of the regressed line. Despite the fact that the data can be described by a linear function (p value of the regression < 0.001), the data appears to actually be better described a nonlinear function. Additionally, the regression had a significant intercept (p value < 0.001). The intercept may be a manifestation of the way the net histogram is developed. By setting the grey levels with negative values to zero, after the preexposure histogram is subtracted from the postexposure histogram, the resulting net histogram may have an artificially inflated brightness. This inflation of the net brightness would contribute to the intercept term of the summary standard curve. The negative intercept term would shift the curve to the right, underestimating the exposure. An alternative is to use the average grey level of the net histogram instead of the calibration grey level to develop the standard curve. This would require no additional effort since the latest version of the VITAE calculating program generates this information. Given the way it is calculated, the function relating average net grey level and net brightness should not have an intercept.

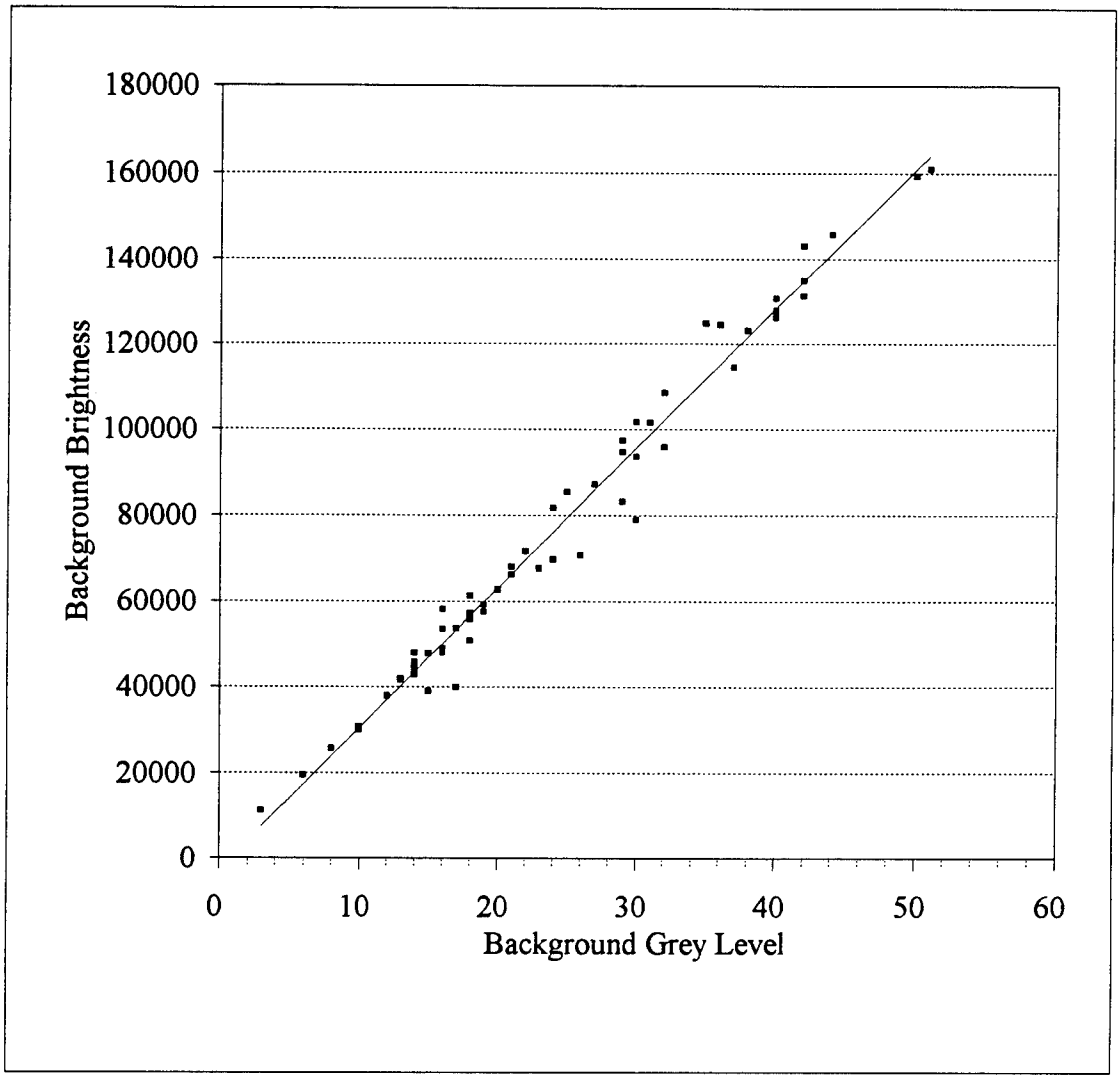

Figure 4.3 Background Grey Level vs. Background Brightness

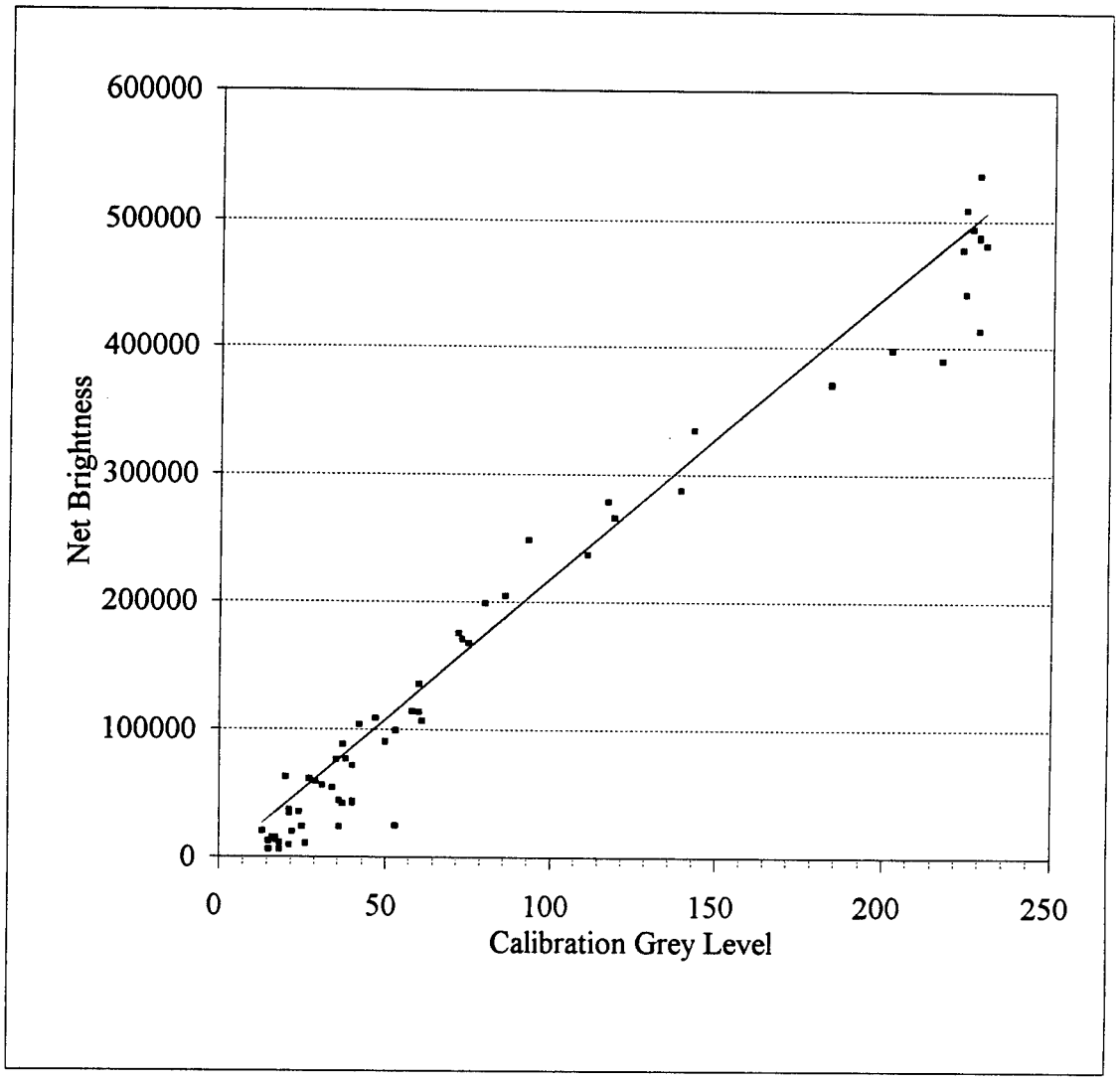

Figure 4.4. Calibration Grey Level vs Net Brightness

The use of the calibration grey level may have another impact on the system. Figure 4.4 reveals an interesting phenomena; there appears to be an upper bound to the relationship between the integrated net brightness and the calibration grey level. It appears that although the system measures a high response in terms of brightness, the calibration grey level does not capture this. Examination of high brightness histograms indicated that as brightness increases, the histogram seem to become left skewed. This shift in the shape of the distribution would cause a rise in the integrated brightness without a corresponding increase in a median-like parameter like the calibration grey level. What this means is that the quenching noted by Fenske et al. (1990) and Black (1993) might actually be partially due to distributional shifts and not the result of true, physical quenching of the tracer irradiance.

4.2.2 Symmetry of Preexposure Histogram

The linear regression of the average BGL and the median BGL (Figure 4.5) indicated both a very strong correlation (R^2= 0.996) and a line that was not significantly different than unity. The slope of the regression line was 1.004, which, when tested for a slope equal to unity, could not be rejected (p value = 0.334). The same was true for a test of the intercept (0.295) not differing significantly from zero (p value = 0.283). These findings, coupled with visual inspection of the preexposure histogram, support the assumption that the histograms are reasonably symmetrical.

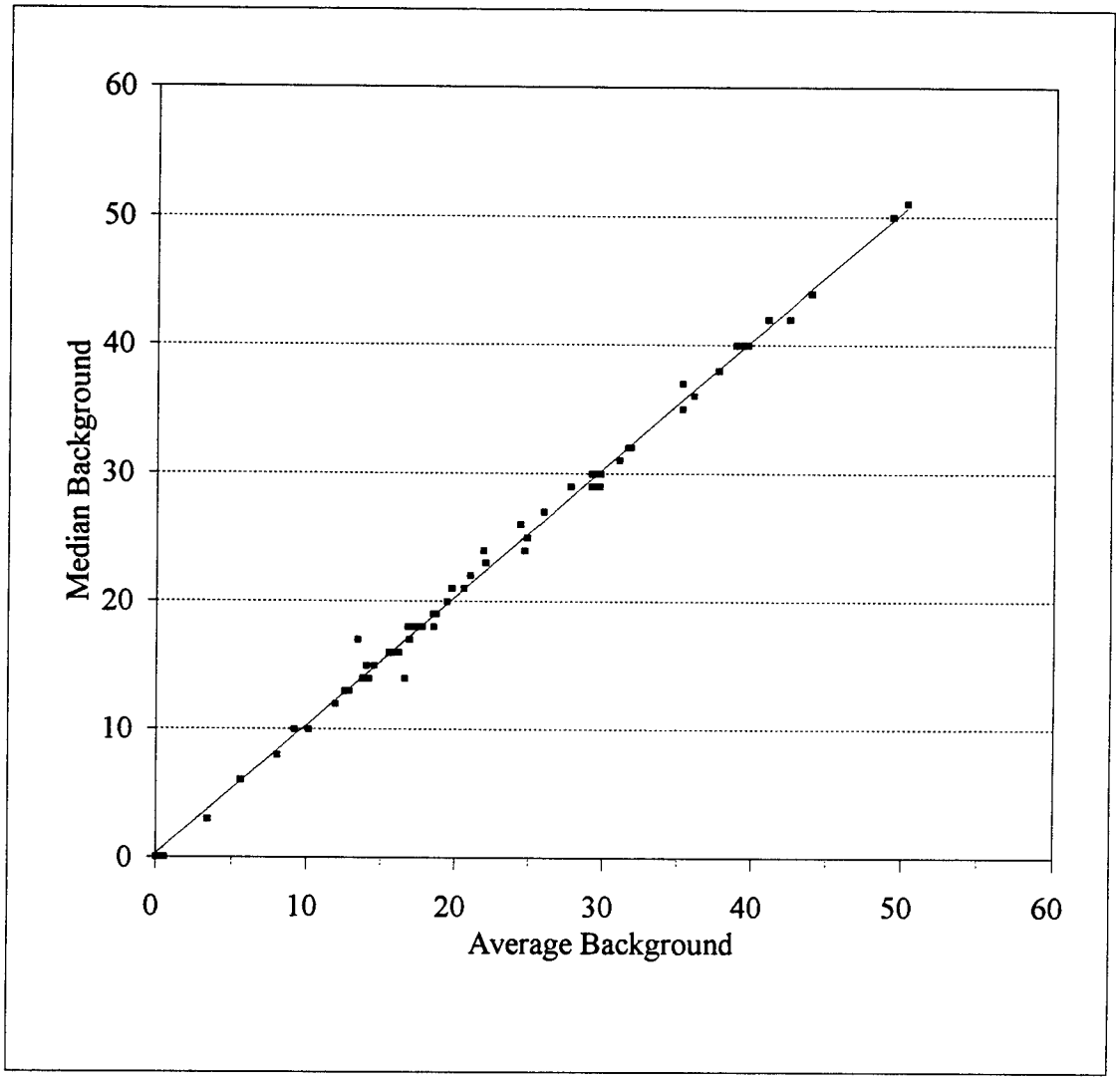

Figure 4.5. Average Versus Median BGL

4.3 *System Response Curve*

The system response curve is the linear regression of the logarithms of the actual loadings of the summary curve images versus the logarithms of the loadings predicted by the VITAE system. The regression line was generated using the doses identified in section 4.1.4 as being reasonably linear (doses 3 thru 10) and is provided as Figure 4.6. The two lowest doses that were not used to construct the summary curve are shown in Figure 4.6, but were not used in the regression of system response.

Initial examination of the response curve indicates that the summary curve approach models calibration exposures fairly well across the range of tracer densities used to develop the summary standard curves. The regression yielded a strong correlation ($R^2 = 0.945$). This is a rather impressive correlation given the fact that the loadings used in the regression spanned six orders of magnitude.

While the slope of the regression line (1.09) deviated less than 10% from unity, it was significantly different than one (p value = 0.01). Although the slope's departure from unity does not appear dramatic, the difference in the untransformed data will be much greater.

On the other hand, the intercept of the regression was rather large (-0.93) and significantly different from zero (p value < 0.001). This intercept is greater than 10% the linear range of the response curve, revealing a significant shift to the right. If the slope were one, this shift would translate to a systematic under estimation of tracer density of about 60%. However, the slope is not one. The identity function and system response curve converge. Table 4.3 illustrates the impact of the slope and intercept on the models prediction of tracer surface densities, given know tracer surface density.

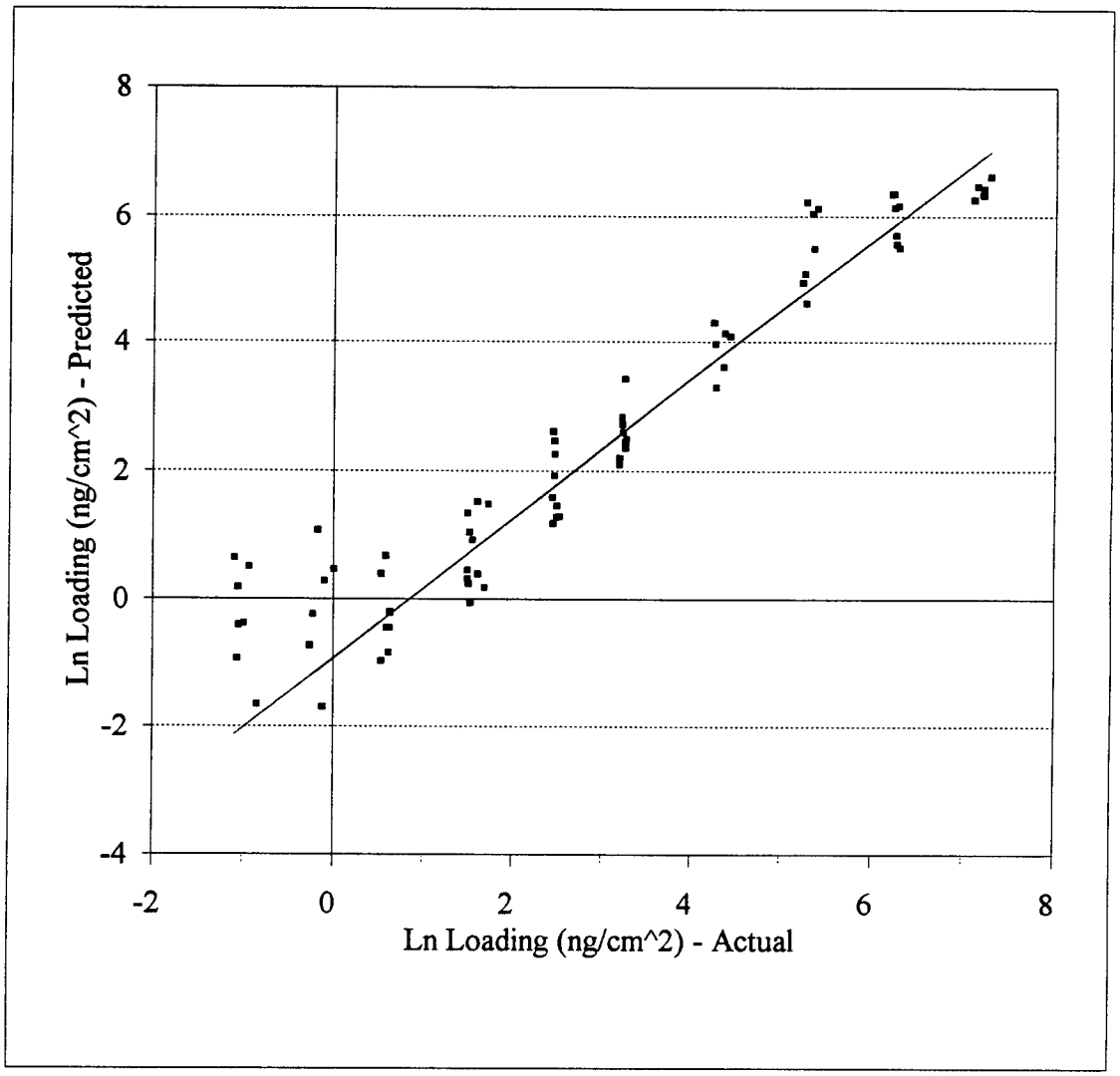

Figure 4.6. System Response Curve

Table 4.3. Examples of System Response for Untransformed Calibration Data

Surface Density (ng/cm^2)	VITAE Predicted Density (ng/cm^2)	Deviation from Actual Density (%)
2.8	1.21	-57.0
5	2.28	-54.4
10	4.85	-51.5
100	59.7	-40.3
1000	734	-26.5

Deletion of the highest dose did not create a significant change in the slope. However, this may be due more to the weight of the other data creating a stable line than the appropriateness of including this dose. All the data points associated with the highest dose fall below the regression line. It appears, looking at Figure 4.6, that quenching is becoming a factor at this loading. The fact that deleting this dose does not cause a significant shift in the slope may be an artifact of the method. The summary curve was constructed including this dose, so the model would reflect the influence of the images at the high dose.

Analyzing the calibration images also bore out the difficulties in evaluating images with average BGLs less than one. Six of the calibration images had average BGLs of less than one. The relative error of these images, for untransformed loadings, ranged from 1265 to 2.2×10^7 percent. The VITAE predicted loadings of these images were considered aberrant and were not included in any analysis involving predicted loadings.

4.4 *Normality of Response Curve Residuals*

Before the assumptions of independence for system parameters and system response can be evaluated, it must be shown that the assumption of normality for the residuals of the response is reasonable. Figure 4.7 provides a probability plot (probit scale). While not truly linear, it would appear reasonable to fit a line to the data. Using the residuals of the response curve and testing for normality with Lilliefors test, yield a Lilliefors' probability (2-tail) of 0.26. While the probability was not exceeding high, the assumption of normality was not rejected.

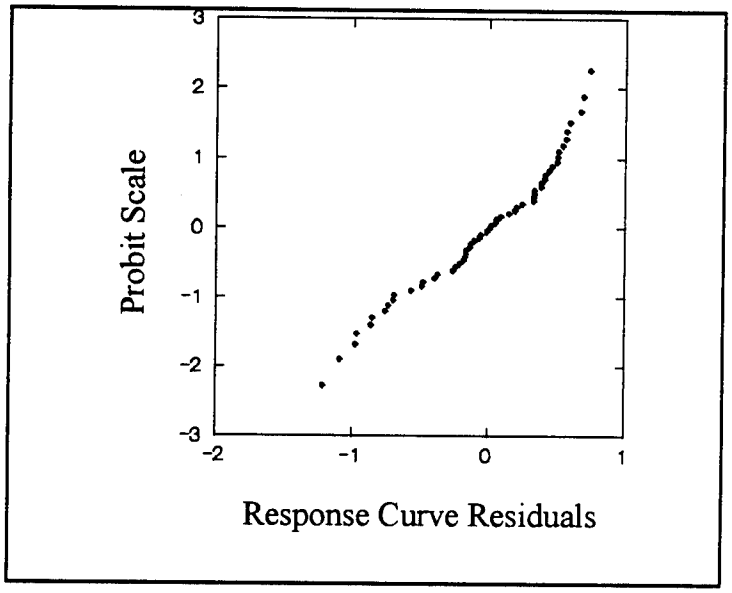

Figure 4.7. Probability Plot of Response Curve Residuals

4.5 *Independence of Samples*

Analysis of variance for the variables identified in subsection 2.5.3 indicate that the location of the sample does not contribute significantly to the variability of the system response. Evaluating the influence of anatomical location by using all eight locations as

different groups, yielded an R^2 of 0.127 and a p value of 0.432. If the dorsal portion of the hand, the forearm and the upper arm are consider similar surfaces, but dissimilar to the palm, grouping the areas in eight different categories might suppress a truly significant influence of anatomical location on system response. This was investigated by dividing the sample locations into just two group, palm and other surfaces. Analysis of variance on these categories reinforced the assumption that the system response is independent of anatomical location. This analysis yielded an R^2 of 0.019 with a p value of 0.304

On the other hand, subject differences described a significant portion of the variability, yielding an R^2 of 0.453 and a p value of less than 0.001. There is a question of valid analysis here. It would probably be more appropriate to perform the analysis with subject and BGL nested, since the variability might be more correctly attributed to skin pigmentation than some other factors of intersubject variability. Unfortunately, the statistical package employed could not perform the analysis on nested, dissimilar variables (one continuous and one categorical).

4.6 *Assumptions of Summary Curve Application*

As shown in subsection 4.2.2, applying the standard summary curve using the mean BGL, when the median BGL was used to develop the summary curve, should not create an invalid condition. The regression of median and mean BGLs yielded a line whose parameters (slope and intercept) did not differ significantly from an identity line (slope = 1, constant = 0).

The VITAE system also predicts the loading well across the linear range of the of the response curve. A linear regression of the loadings versus the residuals of the response curve validates that the performance of the system is not dependent on loading in this range. The regression produced a slope that was not significantly different from zero (p value = 0.96).

Analysis of variance for the effects of logarithm of the median BGL (this is the transform that was used to construct the model) on performance of the system revealed that the summary curve approach does not completely correct for the effects of background irradiance. The analysis yielded an R^2 of 0.80 (p value < 0.001). If the BGL was independent of any other variables, it would describe 80% of the variability of the response curve residuals. But two things should be considered when judging the affect of this seemingly dramatic correlation. First, the BGL is not independent of subject and a portion of the effect may be related to other factors of subject variability. Considering the fact that the correlation coefficient of the effect of BGL is considerably greater than that of effect of subject (0.45), it would appear that the reverse is probably true (i.e. variability described by subject is more correctly attributed to BGL). The second issue that should be considered is that this measure does not relate to relative performance. To answer this, the variability without the summary curve correction for BGL and/or the variability with some other approach must be known. This issue warrants investigation and should be a central issue in any further efforts to evaluate or enhance the accuracy of the system.

4.7 *Operating Range of Summary Standard Curve*

Before Equation 2.6 was applied to determine the detection limit an analysis of variance was performed to validate that the assumption that the response curve residuals were not dependent on the dose applied and could be pooled. This analysis produced a p value of 0.31, validating the assumption. The standard deviation of the pooled residuals was 0.531. Using this and Equation 2.6, the detection limit of the summary standard curve for the operating conditions of this study was determined to be 2.8 ng/cm^2. This corresponds to

loadings that would be produced by the application of a dose whose concentration lies between the third and the fourth dose. This falls within the linear range of the response curve, making it the lower limit of quantification for the system.

As noted earlier, deletion of the highest dose did not significantly impact the response curve. Additionally, the data points corresponding to the high dose did not fall outside the 95% confidence interval of the system response. The quantification limit of the system was not exceeded with the loadings used. But, as discussed earlier, this may be due to the method of developing the summary standard curve and not a lack of quenching.

4.8 *Simulated Exposures*

Eight subjects were exposed to tracer to evaluate of the system for performance under varying distribution conditions. All subjects were exposed to both simulated exposures in the same session. Unfortunately, data for three of the subjects were lost due to a tape drive malfunction. Again, image pairs with preexposure integrated brightness greater than postexposure brightness were deleted from the data set for the same reasons discussed earlier.

4.8.1 Evaluation of Dorsal Exposures

For each subject different concentrations of solutions were applied as described in the Methods chapter. Eight applications were made for each subject. The intent was to achieve loadings that started below the detection limit and exceeded the upper limit of the system. The regression for the response curve of the dorsal exposures was developed deleting images whose loadings were below the detection limit or had more than 5% of the pixels in the net histogram exhibiting saturation (having grey level of 255). However, this censored nearly half the data, leaving 48 of 80 image pairs. The remaining images only represented two of the

exposure concentrations used. To have enough data to allow for meaningful analysis, the lower doses were not deleted.

Figure 4.8 shows the response of the system as well as the regression of the logarithm of actual loading versus logarithm predicted loading, which is the response curve for the dorsal exposure. The regression line is described by a slope of 0.65 and an intercept of -0.045, both of which differ significantly (p values < 0.001) from the parameters of the calibration response curve. These regression parameters should not be considered reliable. This is due to the fact that the regression contains data below the detection limit of the system and the regression data is clustered in two distinct groups at either end of the data range. However, the data does suggest that under these conditions, the system responded differently than it did for the calibration exposures. This evident if only the exposures associated with the upper cluster are considered (they fall with the range densities for linear system response). In this cluster of surface densities, the predicted loadings for all five subjects and all exposures were below the actual loadings. The same is not true for predicted loadings of similar tracer densities for the system response curve. Additionally, the mean-square of the residuals increased more than three fold over the calibration response data, increasing from 0.318 to 1.396. This dramatic increase in variability is evident in Figure 4.8. The data points that fall well below the other data and the regression line, correspond to a subject whose BGL was considerably darker than the remaining subjects.

The distribution of the tracer was not as intended. The acetone solution wicked considerably when the skin was contacted with the pipettor. As a result, tracer was not distributed in a pattern of fine, round dots. Rather, it appeared, in the images, as small

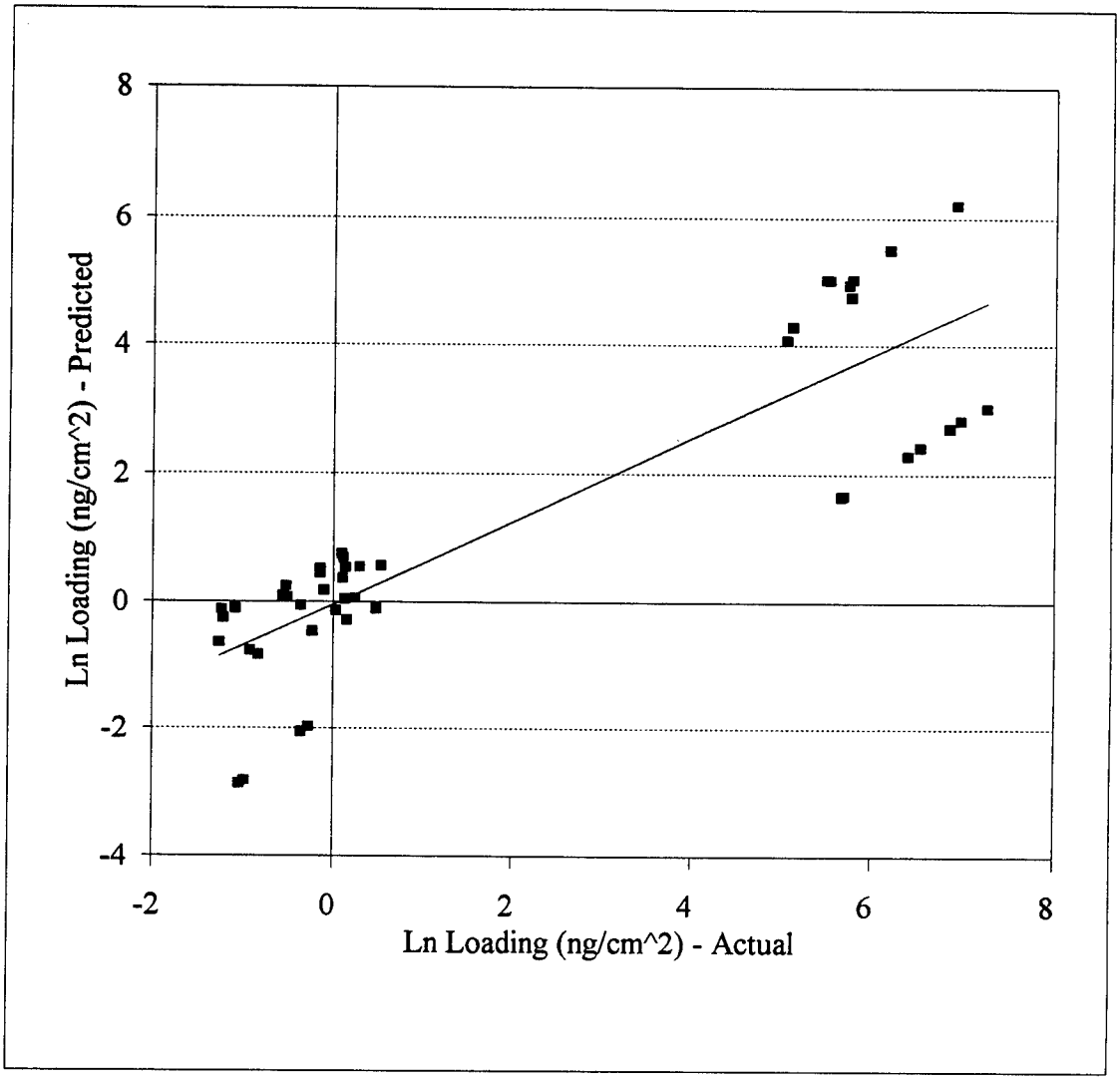

Figure 4.8. Response of Dorsal Exposures

asymmetrical patches. However, the distribution was still considerably different than the calibration exposures. Further, this may actually mimic true exposures more closely than the intended exposure pattern. Liquid aerosols deposited on the skin may wick similarly to the dorsal exposures of this study.

4.8.2 Evaluation of Palm Exposures

The simulated exposures to the palm of the hand were distributed across the range of loadings much more evenly than the dorsal exposure. This was due mainly to the method of application. The exposure pattern also appeared as intended, with relatively large areas of continuously exposed areas. The areas of exposure were the tip pads of the fingers and the portion of the palm just below the first finger joint. The brightness appeared nonuniform for exposed areas, with the intensity varying from low at the edges to high in the center of the exposed areas.

The distribution of doses allowed the response curve regression to be performed without using images with loadings below the detection limit or images with greater than 5% of the net histogram pixels exhibiting saturation. Figure 4.9 illustrates the resulting response curve. The lower doses (below a log transformed value of 1.0) are show in the figure, but not used in the regression. The slope of the palm exposure response curve was 0.718, which was significantly less than the slope of the calibration response curve (p value < 0.001). On the other hand, the intercept (-1.204) was not significantly different than the calibration response curve intercept (p value = 0.58). Although the response curve for the palm doses can be described with linear function (p value < 0.01), it appears in figure 4.9 that the data might be better described with a nonlinear function.

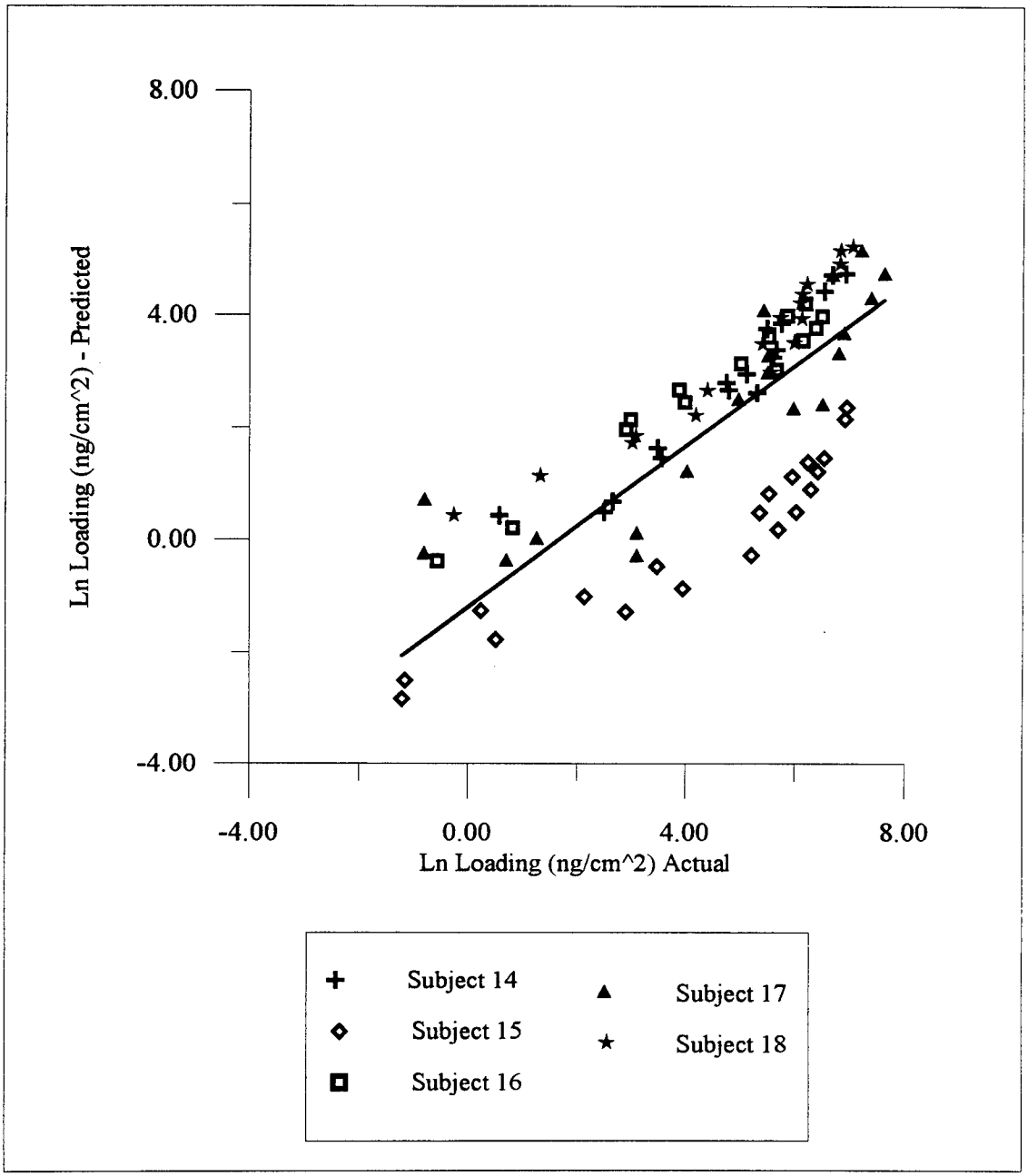

Figure 4.9. Response of Palm Exposures

Again, the logarithmic transformation of the data masks the true performance of the system. The theoretical (unity) response curve and the response curve of the palm exposures diverge. Using the regression line for the palm exposure response, the result of this divergence on the untransformed data is illustrated in Table 4.4.

Along with the large differences between actual and predicted tracer densities and increased variability, the simulated exposures of the palm also dramatically reveal the system's inability to completely correct for background irradiance. Figure 4.9 graphically illustrates this. Subject 15, who had skin complexion considerably darker than the other subjects, produced system response that was very different than the other subjects.

Table 4.4. Examples of System Response for Untransformed Palm Exposure Data

Surface Density (ng/cm^2)	VITAE Predicted Density (ng/cm^2)	Deviation from Actual Density (%)
2.8	0.63	-77.5
5	0.95	-80.9
10	1.57	-84.3
100	8.19	-91.8
1000	42.7	-95.7

4.9 *Potential Causes of Varying System Response*

The simulated exposures produced system responses that were considerably different than both the theoretical identity line and the response to the calibration exposures. The reason(s) for this varying response could not be identified with the approach used to evaluate the

system. But, the process of evaluation revealed several potential areas of concern that might contribute to the variations in response. These concerns might be due to either the construction and application of an inappropriate model or/and the effects of distributional differences.

The construction of the summary standard curves is equivalent to a rather complex mathematical model, providing the parameters of a linear curve for logarithmically transformed data. The parameters themselves are based on a functions that include multiple logarithmic transforms as well as untransformed values. The exponential of the equation (Equation 2.2) must be taken to obtain the estimated mass of the tracer. Given the relatively large values of the terms that determine the intercept and the fact that the intercept is negative for median BGL above two, there is the potential for the intercept to overwhelm any contribution from the slope term. Any problems associated with this might not be easily detected when the images evaluated by the system are similar (or the same) as the images used to construct the summary curve. However, when the distribution of tracer is different from the calibration images, the inappropriateness of the model may become apparent.

Another possible contributor to the variations in system response may be due not to the modelling approach, but to the differences in tracer fluorescence. Differences in fluorescence might arise from differences in tracer surface distribution. The calibration exposures were performed to achieve even, uninterrupted surface densities of tracer. As a result there was relatively little exposed/unexposed border length compared to the size of the exposed area. The same is not true for the simulated exposures. In these cases the exposed areas were not contiguous and ratio of border length to exposed area was greater than the calibration

exposures. Since the surface of the skin is not specular, a significant portion of the light emitted from a pixel sized area of skin and detected by the camera, might be light emitted from the area of interest and reflected off neighboring skin area to the camera. If neighboring skin areas are bright, as in skin exposed tracer, the neighboring surface would reflect more light than darker, unexposed skin. The result of such a phenomena would be reduced tracer irradiance for exposures with high exposed border length to exposed area ratios. Another difference between the distribution of tracer in the simulated and calibration exposure was the presence of an obvious density gradient. This may have resulted in a significant portion of pixels that contained insufficient amounts of tracer to be detected by the system.

CHAPTER V

CONCLUSIONS

The assumptions of central tendencies and symmetry inherent in construction of the summary standard curve were reasonable, with the exception of the calibration grey level. Despite the considerable amount of effort involved in determining the calibration grey level for each calibration image, the approach yielded a significant intercept when correlated to net histogram brightness. This, coupled with the fact that there appeared to be a upper limit to the brightness that could be represented by the calibration grey level, makes the parameter a less than optimal descriptor of irradiance of exposed pixels.

Optimizing the correlation coefficients of the BGL-specific response curves to determine the linear range the summary standard curve fails to reliably identify tracer densities that outside the linear range. The highest calibration exposure appeared to fall above the range of linear responses for the system, but optimizing the correlation coefficients of the individual BGL-specific response curves failed to identify this data set for censoring.

Although the system response curve had a high R^2 (.945), the response differed significantly from the theoretical identity curve. This may be due to the use of the calibration grey level and use of linear regression for possibly nonlinear data. The evaluation of the system response curve also revealed that the method is very sensitive to small changes in the parameters of the summary standard curves.

Evaluation of system response revealed that the response of the system is independent

of anatomical location of the imaged surface. In contrast, the summary curve approach does not completely correct for the effects of background brightness. Eighty percent of the variability of system response for calibration exposures could be described by the median BGL.

Evaluation of exposure to tracer with distributions that simulate some possible workplace exposures revealed that the VITAE method is not robust with respect to variations in tracer surface distributions. The method yielded estimates of tracer densities that were significantly different than the estimates obtained under calibration conditions. Additionally, there was a rise in the variability of the system response. The result was a dramatic underestimation of tracer densities, especially at the high end of the calibrated response range.

CHAPTER VI

RECOMMENDATIONS

The sole intent of the summary standard curve approach is to correct for the effects that background irradiance the skin on the irradiance of the fluorescent tracer. It is apparent of the method does not completely correct for this effect. However, it is still unknown as to what degree, if any, this effect is reduced. This should be determined before any further VITAE work using this approach is conducted. This could be accomplished by developing a calibration curve that does not correct for background irradiance (e.g. relating net histogram brightness to tracer mass) and comparing the results of such an approach to the results of the summary standard curve approach.

The effects of distribution on tracer irradiance should be explored and if the effect is determined to be significant, a means of adjusting for the effect must be sought. The effect might be explored by comparing the net brightness for several distinctly different tracer distributions with total tracer mass held constant. Artificial surfaces, where distinct boundaries can be developed and controlled, might also be used to explore the effects of boundary conditions.

An alternative for the calibration grey level should be sought to better describe exposed pixel distributions. One obvious candidate is the average net histogram grey level. Any alternative parameter can be tested comparing system response using the new candiate for describing exposed pixel distributions and response using the calibraiton grey level..

The distribution of pixels in the calibration image histograms (preexposure, postexposure,

and net) are all described by measures of central tendency. Use of a more complete description of the pixel distributions in the calibration approach may make the method more robust to changes in surface distributions of the tracer. Use of such parameters as integrated brightness, skewness, or peakness in different combinations should be explored.

GLOSSARY

Brightness (integrated) - The summation of all the grey levels in an image or portion of an image. From the histogram, this is calculated by:

$$Brightness = \sum_{0}^{255} grey\ level \cdot \#\ pixels\ at\ grey\ level$$

Background - Describes an image that represents a skin surface that has not been exposed to tracer. It is associated with some description of the image histogram (brightness or grey level). When associated with grey level, a term associated with the grey level's location in the histogram (median, mean, maximum, or minimum) precedes the use of the word background (e.g. median background grey level).

Calibration Grey Level - A median-like value that describes the distribution of the pixels that are considered to represent areas of skin that are exposed to tracer. It is calculated using calibration images where the distributions of pixels in the postexposure histogram are clearly bimodal, with one mode representing exposed pixels and the other unexposed pixels. The technique is more fully described in Section 2.3.

Grey Level - The digital value associated with a pixel that describes the intensity of light detected by the system. The hardware employed here gives a value from 0 to 255, where the increase in grey level corresponds to a linear increase in light intensity.

Histogram - calculated by the VITAE calculating program using the array of pixel location and grey level. It is the distribution (frequency) of grey level values in an image or portion of an image, represented in tabular form as the number of pixels for each possible grey level. (Rich et al., 1989)

Image - here is refers to the digital representation of the light intensities measured at the surface. The image is a 480 x 512 array. Each cell (pixel) in the array corresponds to a detector in the camera, which in turn corresponds to a finite area on the imaged surface. The analog equivalent is a picture element.

Pixel - is the cell in the image array. It has both two dimensional (height and width) and spectral (grey level) attributes. The number of pixels is set, determined by the hardware of the system. The spatial dimensions are a function of camera zoom and the distance from the camera to the surface imaged. Displayed in analog, it is the picture element of the image.

Summary Standard Curve - The VITAE calibration tool. It provides a linear relationship between the *ln* of the postexposure grey level and the *ln* of the tracer surface density, given the median background grey level. The summary standard curve is comprised of two lines, one describing the slope of the aforementioned relationship and the other describing the intercept. See section 2.3.

Video Ramp - Is the relationship between detected light intensity and assigned grey level. In

the case of this system, the video ramp is linear. If the grey level were plotted against light intensity, the resulting function would be linear.

LIST OF REFERENCES

Archibald, B.A.; Solomon, K.R.; Stephenson, G.R.: A New Procedure for Calibrating the Video Imaging Technique for Assessing Dermal Exposure to Pesticides. Arch. Environ. Contam. Toxicol. 26:398-402 (1994)

Bird, M.G.: Industrial Solvents: Some Factors Affecting Their Passage Into and Through the Skin. Ann. Occup. Hyg. 24:235-244 (1981)

Black, K.G.: An Assessment of Children's Exposure to Chlorpyrifos From Contact With a Treated Lawn. Dissertation submitted to Graduate School-New Brunswick Rutgers, The State University of New Jersey. (1993)

Burg, A.W., M.W. Rohovsky, and C.J. Kensler, "Current Status of Human Safety and Environmental Aspects of Fluorescent Whitening Agents Used in Detergents in the United States," CRC Critical Reviews in Environmental Control, 7:91-120, 1977.

Buxtorf, A., "Toxicological Investigations With Fluorescent Whitening Agents." in Fluorescent Whitening Agents (R. Anliler and G. Miller eds.) EQS Environmental Quality and Safety (F. Coulston and F. Korte, eds.), Supplement Volume IV G. Thieme Publishers, Stuttgart, 1975.

Ciba-Geigy Limited, "Eye Irritation in the Rabbit TK 10326," unpublished report, Basle, 1975a

Ciba-Geigy Limited, "Skin Irritation of the Rabbit After Single Application of TK 10326," unpublished report, Basle, 1975b

Ciba-Geigy Limited, "Accumulation Test of _____ in the Rat," unpublished report, Basle, 1979.

Ciba Limited, "Acute Toxicity of _____," unpublished report, 1963.

Ciba Limited, "Effect of Prolonged Dietary Administration of TAP 1159 to Rats," unpublished report, Basle, 1964a.

Ciba Limited, "Ciba TAP 1159 Subacute Oral Toxicity in Dogs." unpublished report, Basle, 1964b.

Ciba Limited, "Patch Testing with Ciba Compounds 1446, 1159, 33185," unpublished report, Basle, 1964c.

Ciba Limited, "Effects of _____ Administered Orally to Rats Over a Two-Year Period," unpublished report, Huntingdon Research Center, Huntingdon, England, 1969.

Ciba Limited, "Effects of _____ (TAP 1159) Administered Orally to Mice Over a Two-Year Period," unpublished report, Huntingdon Research Center, Huntingdon, England, 1969.

Fenske, R.A.: A Fluorescent Tracer Technique for Assessing Dermal Exposure to Pesticides. Ph.D. Dissertation, University of California, Berkley. (1984)

Fenske, RA.; Leffingwell, J.T.; Spear, R.C.: A Video Imaging Technique for Assessing Dermal Expoure I. Instrument Design and Testing. Am. Ind. Hyg. Assoc. J. 47:764-770 (1986a)

Fenske, R.A.; Wong, S,M.; Leffingwell, J.T.; Spear, R,.C.: A Video Imaging Technique for Assessing Dermal Exposure II. Fluorescent Tracer Testing. Am. Ind. Hyg. Assoc. J. 47:771-775 (1986b)

Fenske, R.A.; Correlation of Fluorescent Tracer Measurements of Dermal Exposure and Metabolite Excretion During Occupational Exposure to Malathion. Am. Ind. Hyg. Assoc. J. 49:438-444 (1988)

Fenske, R.A.; Birnbaum, S.G.; Cho, K.: Documentation for the Second Generation Video Imaging Technique for Assessing Exposure (VITAE System). Department of Environemental Sciences Report, Rutgers University, New Brunswick NJ. (1990)

Fenske, R.A.; Black, K.G.: Toxicolory Review of Uvitex OB Fluorescent Whitening Agent [2,2'-(2,5-Thiophenediyl)-bis(5-tert-butylbenzoazole); CAS 7128-64-5]. Department of Environmental Sciences Report, Rutgers University, New Brunswick, NJ. (1990)

Fenske, R.A.; Lu, C.: Determination of Handwash Removal Efficiency: Incomplete Removal of the Pesticide Chlorpyrifos From Shin by Standard Handwash Techniques. Am. Ind. Hyg. Assoc. J. 55(5):425-432 (1994)

Gloxhuber, C. and H. Bloching, "Toxicological Properties of Fluorescent Whitening Agents," in Toxicology Annual (Charles L. Winek, ed.) Marcel Dekker Inc. NY-Basel, 1979.

Griffith, J.F., "Fluorecent Whitening Agents," Arch. Dermatol. 107:728-733, 1973.

Kirk-Othmer. Encyclopedia of Chemical Toxicology, Third Ed., John Interscience-Wiley, 1981.

McArthur, B.: Dermal Measurement and Wipe Sampling. Appl. Occup. Environ. Hyg. 7(9):599-606 (1992)

OSHA: Occupational Exposure to 4,4'-Methylenedianiline (MDA). Federal Register 57(154):35630-35696 (1992)

Rich, P.M.; Ranken, D.M.; George, J.S.: A Manual for Microcomputer Image Analysis, Department of Biological Sciences, Stanford University, Standford, CA (Los Alamos manual # LA-11732-M) (1989)

Russ, J.C.: The Image Processing Handbook. CRC Press, Boca Raton FL, (1992)

Syracuse Research Corportation. "Information Profiles on Potential Occupational Hazards. Volume III. Chemical Classes Fluorescent Whitening Agents (FWAs)". Prepared for NIOSH, Dec., 1979.

Thomann, P. and L. Kruger. "Acute Oral, Dermal, and Inhalation Studies," in EQS Environmental Quality and Safety, (F. Coulston and F. Korte, eds.) Supplement Volume IV, G. Thieme Publishers, Stuttgart, 1975.

Appendix A

Review of Fluorescent Agent Toxicity - Uvitex OB

This review was taken and adapted from Fenske and Black (1990).

The fluorescent compound used as a tracer in this study belongs to a class of chemicals referred to as fluorescent whitening agents (FWAs). The FWAs (also called optical brighteners or fluorescent brightening agents) are widely used in textiles, detergents, papers, and plastics to achieve a bright white color. The FWAs absorb light in the invisible ultraviolet region and emit light in the visible (usually blue to blue-violet) region. The net effect is an addition of visible light to the substrate, making the substrate appear brighter (Kirk-Othmer, 1981). The FWAs generally have moderate to low acute toxicity. Many FWAs have been tested for chronic effects and do not appear to be mutagenic, carcinogenic, or teratogenic to experimental mammals. The compounds in general have not been shown to cause dermal irritation or sensitization in humans (Syracuse Research Corporation, 1979). of the estimated 45,000 metric tons of FWAs produced worldwide in 1975, 20,000 metric tons were used in detergents (Kirk-Othmer, 1981). FWAs are incorporated into detergents to adsorb onto clothing during laundering and maintain fabric whiteness.

Uvitex OB is not used as a detergent additive. Uvitex OB is the trade name for 2,2'-(2,5-Thiophenediyl)-bis(5-tert-butylbenzoxazole) (CAS 7128-64-5). This FWA is approved by the FDA as an optical brightener in food wrappers (21 CFR 178.3297(e)) and

is exempted from tolerances by the EPA, when applied to growing crops (40 CFR 180.1001(d)). It can be used as a fluorescent quality control agent for surfactants used in pesticide applications. Although these uses do not involve skin contact, the studies done to obtain federal approval for the uses provide a good toxicological database. The results of these studies were obtained under the Freedom of Information Act and reviewed.

The short-term studies revealed a rat oral LD_{50} of greater than 10 g/kg (Ciba Limited, 1963; Thomann & Kruger, 1975). An accumulation study using rats reported no toxic symptoms, gross organ changes or changes in body weight gains when Uvitex OB was administered at doses of 0.025 and 0.25 mg/kg/day for 28 days. Tissues analyzed at the end of the study showed a negligible accumulation in the liver, brain, eyes, blood, fat of the testes, and fat storage tissue (Ciba-Geigy Limited, 1979). In one subacute oral study, rats were treated with concentrations of 50 ppm (2.5 mg/kg/day), 5000 ppm (250 mg/kg/day), and 50,000 (2,500 mg/kg/day) Uvitex OB in their diet for 14 weeks. After seven weeks of treatment, the high dose group showed no symptoms; the dose was increased to 100,000 ppm (5,000 mg/kg/day). No toxic symptoms or mortalities were reported in any group. No difference was found among the groups mean food consumption or body weight gains. Terminal urinalysis, hematology, gross and microscopic histopathology showed no treatment related differences. Differences in organ weights were observed among the treatment groups. The liver, kidney, adrenals, and ovaries appeared to be enlarged at various dose levels but, since no dose-response effect was observed, the differences were not considered to be related to the treatment (Ciba Limited, 1964a).

An oral study was also conducted with beagle dogs (Ciba Limited, 1964b). Dogs were fed concentrations of Uvitex OB in their diet equivalent to 2.5 mg/kg/day, 250 mg/kg/day, and 2,500 mg/kg/day for three months. No deaths were observed; no differences in weight gains or food consumption were noted. The only symptoms noted were loose stools in the intermediate and high dose groups. Terminal hematology showed no differences among the groups; terminal biochemistry and urinalysis showed scatter abnormalities in the dogs at various levels. No consistent abnormalities were observed in the microscopic histopathology. Organ weights varied considerably, but no difference could be attributed to treatment.

Effects of skin contact were tested both in rabbits and humans. In one study, 0.1 g of the material was placed in the conjunctival sac of the eye of six rabbits. The eyes of three rabbits were rinsed after 30 seconds. The eyes were examined at 1,2,3,4, and 7 days after exposure and irritation was noted (Ciba-Geigy Limited, 1975a). In another study, the sides and back of six rabbits were shaved and one side was scarified. Gauze patches soaked in Uvitex OB were applied to both sides and covered for 24 hours. No irritation was noted when the patches were removed or upon examination 48 hours later (Ciba-Geigy Limited, 1975b). Another study reports that application of technically pure Uvitex OB to rabbit skin resulted in minimal skin irritation (Thomann & Kruger, 1975).

In human irritation and sensitization studies, patches were soaked in 0.5% and 1.0% mixtures of Uvitex OB and soft white paraffin were applied to human subjects for 48 hours. No primary irritation was noted. A second application was made 2-3 weeks later for an additional 48 hours. Upon removal of the second patch, no sensitizing reactions

were noted. A total of 102 people were tested at both application strengths (Ciba Limited, 1964c). In another study, a 10% concentration of Uvitex OB in a detergent solution was tested in 64 human subjects. Nine applications were made over three weeks followed by a challenge application 2 weeks later. No subjects were sensitized (Griffith, 1973).

Two chronic studies were also conducted. In one study, 140 rats were fed Uvitex OB at a concentration of 1000 ppm in their diet for two years (Ciba Limited, 1968). No differences in growth performance, mortality rate, food consumption, terminal hematology, biochemistry, urinalysis, histology, and total and differential tumor incidence between the treated and control groups were recorded. Fluorescent material was noted in the body fat and eyes of the treated animals. Optic lens opacities in the treated animals were noted in excess incidence of that noted in the controls, although the numbers were small. Liver enlargement was noted in treated males although no evidence of altered histology, serum alkaline phosphatase activity, or serum glutamate pyruvate transaminase activity was observed.

A chronic study was conducted in which 104 mice were fed 1000 ppm Uvitex OB in their for one year (Ciba Limited, 1969). The mice were observed for an additional 26 weeks. Reproductive performance was observed after 36 weeks of treatment. Treatment continued through the F_1 generation. The progeny of the F_1 generation were reared to maturity under treatment, the sacrificed. No effect of treatment was observed in reproductive performance, litter parameters, or morphological abnormalities. Mortality rates, growth, food consumption, and tumor incidence were comparable between the

treatment and control groups. Fluorescent deposits were observed in the adipose tissue of the treated animals. A marginal increase in liver weight was observed in treated males. Again no histological findings correlated with the increase weight. Four of the treated males had large liver tumors; if these were excluded from analysis, no significant difference in liver weights were found. The researchers concluded that there was no evidence that Uvitex OB may be carcinogenic.

Several estimates of skin contact to FWAs used a detergent additives have been made. One study attempted to measure the deposition of FWA on skin from using FWA-containing detergents for dishwashing. Six subjects placed one hand in an FWA-detergent solution for 15 minutes, three times a day for six consecutive days. The average maximum deposition was 2 ug/cm^2 (Burg et al, 1977). Assuming a surface area of 500 cm^2 for both hands, this deposition results in a total deposition of 1 mg. Other estimates of adsorption of direct hand contact of detergent solutions are 0.1 mg on both hands (Buxtorf, 1975) and 0.07 to 0.17 mg (Gloxhuber & Bloching, 1979). A survey was done to determine the fluorescence on the hands of 104 housewives. Two housewives used FWA-containing detergents for dishwashing; they had an average of 0.03 ug/cm^2 (est. 0.015 mg total). The average fluorescence for those using FWA-containing detergents for laundry was equivalent to 0.106 ug/cm^2 (est. 0.053 mg total). Those not using FWA-containing detergents has a fluorescence equivalent of 0.086 ug/cm^2 (est. 0.043 mg total) (Burg et al., 1977). FWAs may also adsorb to the skin through contact with laundered clothing. One study found a transfer of 0.07 ug FWA/cm^2 from 48 hours of contact with a whitened fabric. Assuming a covered body surface of 1.5 m^2, a total of 1.05 mg would be deposited

(Burg et al., 1977). Another estimate for transfer from whitened clothing is a range of 0.05 to 1.7 mg/day; although a range of 0.005 to 0.085 mg/day was thought to be more realistic (Buxtorf, 1975)> In contrast to these estimates, on survey of backs and feet found no fluorescence, indicating a lack of transfer from socks and shirts (Burg et al.,1977).

Appendix B

Copy of Subject Consent Form

UNIVERSITY OF WASHINGTON

CONSENT FORM

INVESTIGATION OF SKIN DEPOSITION AND DETECTION PROPERTIES FOR FLUORESCENT WHITENING AGENTS

Investigator: Richard Fenske, PhD, MPH, Associate Professor
Department of Environmental Health, 543-0916

Student Investigator: Keith M. Groth, Graduate Student
Department of Environmental Health, 685-9299

24 HOUR EMERGENCY TELEPHONE NUMBER: 206-523-9799

PURPOSE

The purpose of this study is to evaluate an imaging technique developed to measure skin exposures to chemical substances which cannot be seen with natural light. This technique could be useful to workers who are exposed to chemicals and other substances in their work, e.g., agricultural workers, construction workers, laboratory workers, pharmacists. The technique uses a fluorescent compound known as Uvitex OB. This compound is widely used as a brightener in clothing, detergents and plastics (e.g., plastic food wrap). Although this compound cannot be seen under natural light, it can be seen under blacklight. Adding trace amounts of this fluorescent compound to chemicals that workers are exposed to, may provide a method to evaluate skin exposure to workplace chemicals.

There is no benefit of the subjects who participate in this research. The information gained may be of future benefit to society by providing a better method of measuring skin exposures to chemicals.

PROCEDURES

If you agree to participate, you will be asked to touch surfaces (glass tubes or plates) that have been treated with the fluorescent compound, Uvitex OB or a small amount of the compound dissolved in acetone. You will be asked to contact the surface briefly with your hands or several drops of the tracer/acetone mixture will be applied to your hands. Video images of the hands will be collected prior to and about 30 minutes after application of the tracer. The imaging procedure involves placing your hands under ultraviolet light, a blacklight, to illuminate the skin while taking photographs with a computer imaging system. These studies will take about 1 hour. You may participate in one to several sessions (up to about five). The number of sessions determined by the length of the study

and the mutual convenience of both you and the investigators. Volunteers will be asked to thoroughly wash their hands with soap and hot water directly after the session.

PHYSICAL RISK AND DISCOMFORT

The levels of acetone exposure in this study are very low and not expected to cause any harm. At much higher concentrations or prolonged exposures, side effects such as nose and throat irritations or skin irritations can occur. No risks are associated with exposure to the fluorescent tracer, since the compound is not considered toxic (harmful). The longwave ultraviolet light is not considered harmful, but in some cases may cause discomfort to the eyes. You will be provided with UV-A shielding glasses during image collection. Photographs made during the sessions will not identify any participant.

OTHER INFORMATION

Your identity will not be retained in the data for this study, and no records will be kept as to specific participants. The results of this study will be published in scientific literature, but only in summary form so that no individual data can be identified with any participant.

Participation is voluntary. You may choose not to participate and you may withdrawal from the study at any time without penalty or loss of benefits to which they are otherwise entitled.

Investigator's Signature _____ Date _____

SUBJECT'S STATEMENT

The study described above has been explained to me, and I voluntarily agree to participate in this activity. I have had an opportunity to ask questions and understand that further questions I may have about the research or about subject's rights will be answered by the investigator listed above.

Signature of the Subject _____ Date _____

Copies to: Subject
Investigator's File

APPENDIX C

Glass Tube Elution Efficiency Study

Purpose

To determine the recovery efficiency of Uvitex OB from glass test tubes using toluene as the elution solvent.

Method

The following method of spiking and recovering tracer from glass test tubes was adapted from a method of recovering pesticides from test tubes developed by Fenske and Lu (1993).

Spike Technique

Test tubes (KIMAX, 127 mm x 16 mm i.d.) were spiked using a solution of Uvitex OB and acetone. All spikes were performed using 50 μl of solution and a positive displacement micropipettor. The mass of Uvitex OB applied to the glass tube was varied by varying the concentration of the Uvitex OB/acetone solution. Uniform application was be accomplished by incrementally rotating the tube while releasing the pipet volume. The pipet was drawn back and forth in a zigzag pattern down the facing length of the tube from just under the label to about a centimeter short of the tip. Solution was released form the pipet at such a speed that the acetone evaporated without running. About one sixth of the pipet volume is released during application of the spike to this "face". The tube was rotated about one sixth of a turn and another sixth of the volume applied. This was repeated until the tube was evenly covered and the pipet volume was emptied. To achieve complete and consistent dispensing of the pipet volume, care was taken ensure that the plunger tip of the pipet was in contact with glass of the tube at the end of dispensing. Solution was applied below the label and avoiding the

tip. This resulted in a spike surface area of approximately 40 cm^2. All tubes were allowed to dry at least ten minutes before elution. Recovery efficiencies were determined for five concentrations that span the anticipated concentrations for doses delivered by contact with spiked test tubes.

Tube Elution

The test tubes were eluted by slowly pouring the toluene from a 30 ml tilting repeater dispenser over the spiked tube that was held about 30° from vertical. As the toluene was poured over the tube, the tube was slowly rotated counterclockwise one revolution and then rotated clockwise to the same start position. Tubes were eluted using either one volume of the dispenser (30 ml) or two volumes (60 ml). The eluate was collected in glass sample jars with foil lined lids. Samples were capped and shaken thoroughly. If samples were not analyzed immediately, they were stored in the sample jars in a freezer (normal temp.: -25 C).

Control Samples

For each spiked concentration four control samples were made. Control samples were made by directly spiking the same volume and concentration that used for test tube application, directly into four separate samples jars. The same pipet used to spike the tubes was used for the control samples. Again, to achieve complete and consistent application, the plunger end of the micropipettor was touched to the inside glass of the sample jar at the end of the pipet volume discharge. Either 30 or 60 ml of toluene was added to the sample jar (depending on the eluant volume used for the samples) using the same tilting repeater dispenser that was used for the elutions. The controls were capped and shaken thoroughly. Controls were treated the same as their corresponding samples, stored or analyzed at the

same times.

Sample Analysis

Samples will be analyzed using a Turner Model 430 Spectrofluorometer. The spectrofluorometer was set with the excitation frequency at 355 nm and emission measured at 450 nm. The spectrofluorometer was calibrated immediately before sample analysis using standard solutions of Uvitex OB and toluene.

Results and Discussion

Table D.1 provides a summary of the elution efficiencies determined for various spike masses. Using two 30 mL elutions, as opposed to a single elution, did not significantly increase the elution efficiency for either the 28 mg/L, 50 uL spike or the 1196 mg/L, 50 uL spike (p-values > 0.2). But, two 30 mL elutions, instead of one, did significantly increase elution efficiency for the 197 mg/L, 50 uL spike (p-value < 0.05). Elution efficiency was not found to be a function of spike mass for either the single elution (p-value > 0.3) or the double elution. (p-value > 0.9).

Conclusions

Although using two elutions only increased efficiency for one spike mass, using two elutions consistently increased efficiency. For this reason as well as the fact that using two elutions should improve consistency since it will allow for recovery of any tracer that might have been missed due to a poorly performed first elution, two 30 mL elutions will be performed the for recovery of tracer form glass test tubes. The exception to this is when using two elutions creates the potential for the concentration of the elution to be less than the

Table D.1: Summary of Test Tube Elution Efficiency

Con. Spike (mg/L)	Samples			Controls			Elution Volume (mL)	Recovery Efficiency (%)
	Avg. Mass (μg)	N	CV	Avg. Mass (μg)	N	CV		
2.8	0.147	6	0.07	0.140	4	0.02	30	105.2
28	1.44	6	0.02	1.41	3	0.02	60	102.5
28	1.41	6	0.03	1.40	4	0.03	30	100.4
197	10.17	6	0.02	9.87	4	0.01	60	103.1
197	9.92	6	0.02	*	--	----	30	100.5
1196	59.41	6	0.02	59.80	4	0.02	60	99.34
1196	59.05	6	0.01	*	--	---	30	98.74
1811	92.67	4	0.03	90.58	4	.01	60	104.61

* Used the values for the control with 60 ml eluant.

calibration range of the spectrofluorometer.

Expect for one spike mass, elution efficiencies were greater than 100%. This is possibly due to the loss of toluene to evaporation during the process and to the toluene remaining on the test tube due to surface tension. The average recovery efficiency for elutions using two 30 mL volumes was 102.4 %. Since this is near what appears to be typical the coefficient of variation for the different spike masses, no correction will be applied to the masses determined using this method.

Appendix D

Determination of Transfer Coefficient

Purpose

To determine the percentage of tracer transferred from a spiked glass tube to a subjects hand when the tube is gripped by the subject. The data was used to estimate doses delivered to the hands of subjects during simulated exposures.

Method

The same test tubes described in Appendix C were spiked in the same manner as described in the Appendix C. Subjects were asked to grip the test tubes, contacting the tube first with the outside blade of the hand. The spiked test tubes were resting upright on pegs and subjects were asked to establish a firm grip, lift the test tube from the peg, and return the tube to the peg. Total contact time was approximately two minutes. Six tubes were gripped consecutively with each hand. The tubes were then eluted as described in Appendix C and the elutant analyzed using the Turner 430 Spectrofluorometer.

Results and Conclusions

Table D.1 provides the results of the transfer coefficient study. No statistical analysis was performed on the data because only an estimate of the amount transferred was needed. It appears that the typical transfer coefficient is about 0.15. Transfer appears dependent on subject and not on spike mass or mass of tracer already transferred.

Table D.1. Results of Transfer Coefficient Study

Subject	Hand	Spike Concentration (mg/L)	Spike Mass (ug)	Mass Remaining (ug)	Percent Transferred (%)
1	Left	4.12	0.215	0.149	30.48
1	Left	4.12	0.215	0.174	19.05
1	Left	4.12	0.215	0.164	23.81
1	Left	4.12	0.215	0.157	26.67
1	Left	4.12	0.215	0.178	17.14
1	Left	4.12	0.215	0.180	16.19
1	Right	4.12	0.215	0.168	21.90
1	Right	4.12	0.215	0.192	10.48
1	Right	4.12	0.215	0.205	4.67
1	Right	4.12	0.215	0.194	9.52
1	Right	4.12	0.215	0.180	16.19
1	Right	4.12	0.215	0.145	32.38
2	Left	1218	61.11	50.46	17.43
2	Left	1218	61.11	51.70	15.40
2	Left	1218	61.11	49.22	19.46
2	Left	1218	61.11	51.29	16.07
2	Left	1818	61.11	58.32	4.57
2	Left	1218	61.11	57.49	5.92

Table D.1. Continued

Subject	Hand	Spike Concentration (mg/L)	Spike Mass (ug)	Mass Remaining (ug)	Percent Transferred (%)
2	Right	1218	61.11	53.77	12.01
2	Right	1218	61.11	55.42	9.31
2	Right	1218	61.11	53.36	12.69
2	Right	1218	61.11	53.36	12.69
2	Right	1218	61.11	55.42	9.31
2	Right	1218	61.11	51.29	16.07
3	Left	1218	60.83	47.14	22.50
3	Left	1218	60.83	45.62	25.00
3	Left	1218	60.83	45.24	25.63
3	Left	1218	60.83	44.48	26.88
3	Left	1218	60.83	47.14	22.50
3	Left	1218	60.83	45.62	25.00
3	Right	1218	60.83	45.62	25.00
3	Right	1218	60.83	44.10	27.50
3	Right	1218	60.83	44.48	26.88
3	Right	1218	60.83	45.62	25.00
3	Right	1218	60.83	46.00	24.37
3	Right	1218	60.83	46.38	23.75

APPENDIX E

Determination of Pixel Dimensions at 20 mm Focal Length

Purpose

To determine both the vertical and horizontal dimensions that are represented as a single pixel on images taken by the VITAE system. This data will be used to approximate the size of areas of interest on digital images.

Method

The following method was adapted from a method used by Fenske (unpublished) The camera, lights, and subject frame were setup as outlined in Methods section, equipment layout subsection. An image was acquired of a 201 mm x 201mm white art board on a background of black darkroom curtain cloth. Using VTOOLS, pixels of the image were examined. The median grey level of the pixels of the white art board were estimated as were the median grey level of the black background area. The corners of the white art board were estimated by finding the pixel at each corner of the board that had a grey level closest to the average of the white and black area medians. The coordinates for each corner was recorded and the dimensions of each pixel found using the relative positions of each corner.

Results and Discussion

Determination of border corners

- Grey level of corners.
  - -- Median grey level of white art board: 9.
  - -- Median Grey level of black background: 184.

-- Border corners selected for pixel nearest a grey level of 87.

- Coordinates of the corners of the white art board.

-- Top left: (59,154)

-- Top right: (60,384)

-- Lower left: (345,153)

-- Lower right: (347,384)

Determination of pixel area

- Calculation of pixel dimensions.

-- Horizontal target dimension (pixels):

L = ((384 - 154)+(383 - 153)/2 = 230 pixels

Pixel Length = 201 mm/230 pixels = 0.87391 mm/pixel

-- Vertical target dimension (pixels)

H = (345 - 59)+(345 - 60)/2 = 285.5 pixels

Pixel Height = 201 mm/286.5 pixels = 0.70403 mm/pixel

- Pixel area = (0.87391)(0.70403) = 0.6153 mm^2

- H:L ratio = 0.6281/0.7791 = 0.8056

Conclusions

The manufacturer of the imaging board (Data Translation) list the pixel height to length ration as 5:6 or 0.8333. This is somewhat different that determined using the method outlined. However, Fenske (unpublished) determined a similar ratio (0.8062) using the same approach.

APPENDIX F

Summary Standard Curve Data

Table F.1. Summary Curve Data - Group 1

Subject	Image	Tracer Mass (ug)	Bckgrnd Brightness	Bckgrnd Grey Level	Post Exposure Grey Level	Calib. Grey Level	Mapped Area (pixels)	Mass/ pixel (ng/pixel)	Median Net Hist.	Net Histogram Brightness	Number Pixels
11	RUA	1.528	199	0	4	10	3191	0.479	15	29001	1745
11	LHB	0.514	701	0	0	2	3187	0.161	5	7210	1320
11	RHB	0.036	1154	0	0	0	3156	0.011	4	2295	461
11	RFA	1.528	1836	0	9	15	3293	0.464	18	35195	1943
11	LUA	0.238	222	0	0	0	3322	0.072	2	1862	666
11	LFA	0.238	863	0	0	0	3199	0.074	3	1235	352
10	RHB	10.644	11344	3	92	119	3286	3.239	120	266683	2407
10	LHB	0.017	11522	4	4	5	3029	0.006	6	1749	2630
1	RHB	1.528	19635	6	36	42	3472	0.440	41	104475	2603
4	RHB	10.644	25932	8	92	139	3183	3.344	139	288387	2329
4	LHB	0.238	25679	8	11	13	3174	0.075	15	20928	1400
1	LHB	0.007	23276	9	10	10	2872	0.002	12	9665	811

Table F.2. Summary Curve Data - Group 2

Subject	Image	Tracer Mass (ug)	Bckgrnd Brightness	Bckgrnd Grey Level	Post Exposure Grey Level	Calib. Grey Level	Mapped Area (pixels)	Mass/ pixel (ng/pixel)	Median Net Hist.	Net Histogram Brightness	Number Pixels
10	LUA	0.514	30196	10	24	27	3247	0.158	28	61662	2250
10	RUA	0.007	30742	10	11	12	3040	0.002	15	5903	405
7	LHB	3.940	30763	10	97	117	3010	1.309	117	278966	2432
2	LHB	1.528	37961	12	34	47	3167	0.482	54	109354	2003
6	LHB	0.093	41742	13	13	15	3248	0.029	17	12564	903
2	RHB	0.093	41998	13	15	16	3336	0.028	18	16113	864
5	LUA	0.514	45881	14	24	20	3365	0.153	33	63547	1922
5	LFA	0.036	435237	14	15	15	3127	0.012	17	6137	366
9	LHB	27.102	44679	14	226	228	3240	8.365	228	486505	2747
5	RHB	0.007	43603	14	15	16	3196	0.002	18	8955	494
6	RHB	0.514	48098	14	21	29	3382	0.152	32	59569	1926
5	LHB	0.238	42796	14	19	21	3056	0.078	24	35104	1450

Table F.3. Summary Curve Data - Group 3

Subject	Image	Tracer Mass (ug)	Bckgrnd Brightness	Bckgrnd Grey Level	Post Exposure Grey Level	Calib. Grey Level	Mapped Area (pixels)	Mass/ pixel (ng/pixel)	Median Net Hist.	Net Histogram Brightness	Number Pixels
2	LUA	0.017	49919	15	16	17	3447	0.005	19	12207	678
4	RFA	0.093	39117	15	17	17	2775	0.034	19	13815	706
4	LFA	0.007	36230	15	15	15	2613	0.003	15	2881	208
5	RUA	0.238	47778	15	19	21	3283	0.072	23	37573	1594
8	LHB	0.036	48087	16	17	18	3077	0.012	20	11938	594
1	LUA	1.528	48998	16	62	73	3126	0.489	73	170691	2423
2	RUA	0.036	53618	16	17	18	3397	0.011	20	6252	320
8	RHB	0.036	48423	16	17	18	3078	0.012	21	11737	557
6	LFA	27.102	58192	16	211	226	3585.5	7.559	226	493841	2784
10	RFA	0.093	39979	17	17	17	2975	0.031	20	15877	794
3	LHB	0.514	53778	17	30	35	3167	0.162	36	76790	2061
4	LUA	0.017	45881	17	17	18	3085	0.006	16	3714	226

Table F.4. Summary Curve Data - Group 4

Subject	Image	Tracer Mass (ug)	Bckgrnd Brightness	Bckgrnd Grey Level	Post Exposure Grey Level	Calib. Grey Level	Mapped Area (pixels)	Mass/ pixel (ng/pixel)	Median Net Hist.	Net Histogram Brightness	Number Pixels
11	LHP	0.093	61473	18	21	22	3313	0.028	25	20326	807
1	LFA	1.528	50843	18	66	72	2942	0.519	70	175271	2537
1	RUA	0.514	55853	18	34	37	3138	0.164	37	88658	2326
2	LFA	3.940	57375	18	67	111	3408	1.156	111	237301	2165
8	LUA	0.514	59378	19	31	38	3162	0.163	42	77315	1774
8	RUA	0.093	59201	19	23	24	3162	0.029	26	35694	1343
6	RUA	0.036	57618	19	20	21	3089	0.012	23	9660	445
3	RHB	27.102	62816	20	222	230	3232	8.386	230	481197	2690
6	RFA	0.017	68864	20	20	21	3541	0.005	24	9167	405
2	RFA	0.093	66283	21	23	25	3352	0.028	28	24090	889
6	LUA	0.238	68090	21	28	31	3314	0.072	34	56978	1669
7	LUA	10.644	71669	22	218	223	3405	3.126	223	477397	2504

Table F.5. Summary Curve Data - Group 5

Subject	Image	Tracer Mass (ug)	Bckgrnd Brightness	Bckgrnd Grey Level	Post Exposure Grey Level	Calib. Grey Level	Mapped Area (pixels)	Mass/ pixel (ng/pixel)	Median Net Hist.	Net Histogram Brightness	Number Pixels
8	RFA	0.007	73254	23	23	24	3267	0.002	23	9045	380
7	RUA	3.940	67751	23	137	184	3069	1.284	184	371273	2262
8	LFA	0.036	69902	24	25	26	3188	0.011	29	11019	414
11	RHP	10.644	81791	24	105	143	3308	3.218	153	334871	2212
10	LHP	1.528	85548	25	48	60	3436	0.445	63	135634	2111
7	RFA	3.940	70794	26	148	184	2908	1.355	184	370479	2207
9	LUA	0.093	87373	27	32	34	3340	0.028	36	54925	1507
4	LHP	0.007	100751	28	31	33	3252	0.002	36	19732	545
9	RFA	0.238	94941	29	35	40	3252	0.073	45	71944	1552
9	RHP	3.940	97584	29	60	86	3283	1.200	98	205241	1990
7	LFA	27.102	83317	29	224	224	2996	9.046	224	508824	2497

Table F.6. Summary Curve Data - Group 6

Subject	Image	Tracer Mass (ug)	Bckgrnd Brightness	Bckgrnd Grey Level	Post Exposure Grey Level	Calib. Grey Level	Mapped Area (pixels)	Mass/ pixel (ng/pixel)	Median Net Hist.	Net Histogram Brightness	Number Pixels
9	RUA	10.644	102009	30	196	228	3462	3.075	228	488077	2688
10	RHP	0.238	93829	30	37	40	3150	0.076	48	42783	893
1	LHP	0.093	79043	30	35	36	2649	0.035	41	44696	1059
9	LFA	0.093	101804	31	35	37	3269	0.028	40	42463	1048
4	RHP	0.007	110459	32	35	38	3366	0.002	41	30431	732
6	LHP	0.036	108598	32	34	36	3400	0.011	39	24115	610
1	RHP	0.093	95987	32	38	40	3002	0.031	48	44079	912
6	RHP	1.528	1240918	35	53	80	3537	0.432	89	199022	2087
9	LHP	27.102	124624	36	222	228	3456	7.842	228	536188	2955
7	RHP	0.017	97024	36	38	38	2720	0.006	41	21543	518
3	LUA	0.238	114691	37	46	53	3249	0.073	59	99811	1672
3	LHP	0.514	123234	38	50	58	3269	0.157	63	114966	1785

Table F.7. Summary Curve Data - Group 7

Subject	Image	Tracer Mass (ug)	Bckgrnd Brightness	Bckgrnd Grey Level	Post Exposure Grey Level	Calib. Grey Level	Mapped Area (pixels)	Mass/ pixel (ng/pixel)	Median Net Hist.	Net Histogram Brightness	Number Pixels
3	RUA	3.940	127940	40	158	228	3289	1.198	228	413957	2267
8	RHP	3.940	130809	40	65	93	3315	1.189	100	248763	2169
8	LHP	0.238	126689	40	46	50	3217	0.074	55	91028	1587
3	LFA	0.514	126268	40	67	75	3184	0.161	76	168140	2321
2	RHP	10.644	143140	42	119	217	3371	3.158	217	390215	2193
3	RHP	0.017	134215	42	44	46	3250	0.005	49	44857	915
7	LHP	27.103	131303	42	218	224	3201	8.467	224	442270	2368
3	RFA	0.238	134945	42	53	60	3288	0.072	64	114185	1788
2	LHP	0.514	145793	44	52	61	3295	0.156	70	107252	1482
5	RHP	0.036	159489	50	52	53	3230	0.011	57	25293	444
5	LHP	10.644	161083	51	149	202	3213	3.313	202	398178	2221

APPENDIX G

Effects of Extreme Values on Summary Curves

Table G.1 Effects of Extreme Doses on Linearity

Group or Summary Curve Parameter	N	Average Grey Level	Slope	Intercept	R^2
Using All Concentrations					
Group 1	12	3.17	0.704	3.421	0.374
Group 2	12	16.67	2.428	-3.75	0.714
Group 3	12	15.917	2.601	-4.885	0.87
Group 4	11	18.273	2.676	-5.273	0.933
Group 5	12	25.75	3.087	-7.989	0.862
Group 6	12	33.25	3.231	-8.778	0.838
Group 7	11	43	3.264	-9.272	0.821
Summary Intercept Curve			-5.061	9.154	0.991
Summary Slope Curve			1.019	-0.324	0.972
Deleting Lowest Dose					
Group 1	11	2.64	0.739	3.73	0.576
Group 2	10	12.8	2.034	-2.009	0.922
Group 3	11	16	2.5	-4.444	0.883
Group 4	10	18.273	2.511	-4.524	0.969
Group 5	10	25.8	2.519	-5.113	0.889
Group 6	11	33.364	3.023	-7.723	0.905
Group 7	11	43	3.264	-9.272	0.821
Summary Intercept Curve			-4.531	8.569	0.97
Summary Slope Curve			0.885	-0.124	0.975

Table G.1 Continued

Group or Summary Curve Parameter	N	Average Grey Level	Slope	Intercept	R^2
Deleting Two Lowest Doses					
Group 1	10	2.5	0.713	4.101	0.777
Group 2	10	12.8	2.034	-2.009	0.922
Group 3	9	15.9	2.321	-3.602	0.926
Group 4	10	18.1	2.511	-4.524	0.969
Group 5	10	25.8	2.519	-5.113	0.889
Group 6	10	33.1	2.869	-6.941	0.943
Group 7	10	43.1	2.933	-7.579	0.821
Summary Intercept Curve			-4.167	8.026	0.99
Summary Slope Curve			0.798	0.0332	0.981
Deleting Lowest Dose					
Group 1	12	3.17	0.704	3.421	0.374
Group 2	11	12.54	2.641	-4.387	0.718
Group 3	11	15.91	2.91	-5.806	0.722
Group 4	10	18.1	2.84	-5.825	0.883
Group 5	11	25.46	3.023	-7.754	0.838
Group 6	11	33	3.132	-8.408	0.746
Group 7	10	43.1	3.101	-8.609	0.784
Summary Intercept Curve t			-4.796	8.257	0.791
Summary Slope Curve			0.947	-0.062	0.882

Table G.1 Continued.

Group or Summary Curve Parameter	N	Average Grey Level	Slope	Intercept	R^2
Deleting Lowest and Highest Doses					
Group 1	11	2.64	0.739	3.73	0.576
Group 2	9	12.67	2.028	-2.02	0.846
Group 3	10	16	2.701	-5.05	0.723
Group 4	9	17.89	2.84	-5.82	0.883
Group 5	9	25.44	2.413	-4.7	0.875
Group 6	10	33.1	2.888	-7.21	0.845
Group 7	10	43.1	3.101	-8.61	0.784
Summary Intercept Curve			-4.326	7.913	0.943
Summary Slope Curve			0.832	0.048	0.891
Deleting Two Lowest Doses and Highest Dose					
Group 1	10	2.5	0.7131	4.101	0.777
Group 2	9	12.67	2.028	-2.02	0.846
Group 3	8	16	2.382	-3.788	0.793
Group 4	9	19	2.583	-4.77	0.939
Group 5	9	25.44	2.413	-4.695	0.875
Group 6	9	32.78	2.705	-6.321	0.908
Group 7	9	43.22	2.732	-6.7634	0.967
Summary Intercept Curve			-3.912	0.753	0.982
Summary Slope Curve			0.7347	0.158	0.943

APPENDIX H

Simulated Exposure Data

Table H.1. Simulated Exposure Data - Subject 14

Side	Hand		Actual Mass (ug)	Pixels	Pre Brightness	Pre Median	Pre Average	Post Brightness	Post Median	Post Average	Net Pixels	Net Brightness	Net Median	Area cm^2	VITAE Mass (ug)
P	R	1	0.080	17670	781871	47	44.259	17682	47	45.240	1522	74177	47	108.745	0.094
P	R	2	0.190	17200	751613	46	43.698	789168	47	45.561	2170	112887	55	106.525	0.164
P	R	3	1.532	17320	746346	46	43.092	804878	47	46.006	2508	134359	56	107.595	0.213
P	R	4	3.851	17651	772430	46	43.761	861933	50	48.549	4286	251643	59	109.188	0.471
P	R	5	10.878	14789	670061	48	45.308	865925	58	58.366	6448	457600	66	91.242	1.328
P	R	6	21.306	17271	771231	46	44.655	924369	50	53.559	3514	297470	76	106.144	1.469
P	R	7	27.847	15988	722004	47	45.159	1014331	58	63.171	7712	615187	69	98.751	2.925
P	R	8	28.557	17449	772131	46	44.251	1028312	53	58.973	5121	453617	79	107.238	2.778
P	R	9	70.572	16818	747871	46	44.468	1216935	56	72.389	7317	764382	83	103.389	8.634
P	R	10	100.438	16311	717010	46	43.959	1265589	57	77.596	7135	828295	94	100.307	11.521
P	L	1	0.080	17872	786183	45	43.990	768645	44	43.025	1522	57133	37	109.871	0.043
P	L	2	0.190	17567	767016	45	43.662	759756	44	43.077	1803	67958	36	108.468	0.056
P	L	3	1.289	16939	745958	45	44.038	761868	45	44.564	2524	116298	37	105.141	0.171
P	L	4	3.608	17948	780863	45	43.507	865990	47	48.220	2864	201859	70	110.449	0.566
P	L	5	10.635	16918	759219	46	44.876	905636	46	53.559	5001	391434	80	93.216	1.545
P	L	6	17.176	15160	682676	46	45.031	874519	53	57.697	4492	371488	79	103.991	2.013
P	L	7	22.259	15224	686808	46	45.113	1011823	56	66.655	6104	580994	87	93.358	4.003
P	L	8	28.314	14701	669064	47	45.511	979118	53	66.725	4852	516341	101	90.246	4.257
P	L	9	70.815	14563	665269	47	45.682	1162635	56	80.016	6071	753000	113	89.360	10.019
P	L	10	129.838	16307	727448	46	44.610	1313263	54	80.533	5973	829068	126	100.289	13.894

Table H.1. Continued

Side	Hand		Actual Mass (ug)	Pixels	Pre Brightness	Pre Median	Pre Average	Post Brightness	Post Median	Post Average	Net Pixels	Net Brightness	Net Median	Area cm^2	VITAE Mass (ug)
D	R	1	0.037	13716	329654	24	24.034	342959	25	24.933	1092	32879	30	84.594	0.037
D	R	3	0.111	13443	318367	24	23.683	364467	27	27.110	3969	122901	30	82.681	0.144
D	R	4	0.148	14108	336975	24	23.885	384947	27	27.309	4333	133183	30	86.691	0.154
D	R	5	30.132	14243	343982	24	24.151	1044491	34	73.447	8636	890227	59	87.460	15.818
D	R	6	60.116	15077	357569	24	23.716	1543170	48	102.380	10096	1409206	125	92.700	30.443
D	R	7	90.100	15267	383947	24	25.149	1868428	78	121.594	11615	1748314	156	94.502	40.386
D	R	8	120.084	15460	367917	24	23.798	2015568	103	130.415	11543	1909241	192	95.049	46.098
D	L	1	0.037	15068	342600	22	22.737	359927	23	23.907	1188	34942	30	92.589	0.043
D	L	3	0.111	15414	345417	22	22.409	374694	24	24.358	2284	62220	26	94.606	0.071
D	L	4	0.148	14813	331548	22	22.382	364534	24	24.531	2680	74071	27	91.390	0.083
D	L	5	30.132	15426	340494	22	22.073	900015	30	58.412	6237	677327	85	94.760	11.066
D	L	6	60.116	16285	398376	22	24.463	1354762	37	83.298	8190	1127152	125	100.024	22.422
D	L	7	90.100	15748	346780	22	22.021	1632878	58	103.840	9776	1487543	153	96.710	31.341
D	L	8	120.084	16215	395050	22	24.363	1797487	66	110.888	9654	1606483	185	99.692	36.641

Table H.2. Simulated Exposure Data - Subject 15

Side	Hand		Actual Mass (ug)	Pixels	Pre Brightness	Pre Median	Pre Average	Post Brightness	Post Median	Post Average	Net Pixels	Net Brightness	Net Median	Area Sq cm	VITAE Mass
P	R	1	0.034	17364	464852	27	26.590	499669	29	28.664	1558	59537	37	107.208	0.088
P	R	2	0.119	14853	398258	27	26.813	484846	32	31.925	3584	151968	41	93.401	0.265
P	R	3	0.927	17516	455439	27	26.001	575380	32	32.670	4126	188693	46	108.315	0.396
P	R	4	3.489	17586	462998	27	26.328	618430	32	35.035	3754	214728	54	108.561	0.682
P	R	5	19.749	14920	419415	28	28.111	628829	35	41.444	4150	298589	66	93.315	1.511
P	R	6	27.748	17864	479966	27	26.867	788383	35	43.989	5347	420616	72	110.363	2.523
P	R	7	40.606	17349	461974	27	26.628	784851	33	45.203	4837	432226	81	106.783	3.293
P	R	8	52.006	16706	435588	27	26.074	828505	36	49.620	5698	506775	81	102.687	4.091
P	R	9	63.407	15071	411500	28	27.305	823359	37	54.444	5598	544064	88	93.007	4.004
P	R	10	96.189	15222	415537	28	27.298	1027299	42	67.342	6601	766535	105	93.819	10.041
P	L	1	0.029	15584	376778	25	24.177	400088	26	25.586	1046	37586	37	96.168	0.056
P	L	2	0.163	15839	376211	25	23.782	437935	28	27.626	2754	103653	37	97.491	0.166
P	L	3	1.748	15534	383630	25	24.696	452602	30	29.157	3581	146319	40	95.467	0.266
P	L	4	5.039	15760	379472	25	24.078	465528	29	29.599	3788	166845	42	96.728	0.406
P	L	5	16.925	15029	366114	25	24.361	491894	30	32.697	3918	214895	53	92.521	0.709
P	L	6	27.354	14906	367217	25	24.635	532976	31	35.624	4500	266609	54	92.011	1.097
P	L	7	37.782	14861	368484	26	24.795	567120	30	37.973	4602	312029	64	91.850	1.506
P	L	8	47.725	14536	357133	25	24.569	612005	33	42.336	5163	377051	67	88.905	2.180
P	L	9	60.097	15920	387698	25	24.353	738354	33	46.069	6424	503509	72	98.567	3.328
P	L	10	101.626	16708	386068	24	23.107	960273	34	57.674	7000	728838	89	102.398	8.892

Table H.2. Continued

Side	Hand		Actual Mass (ug)	Pixels	Pre Brightness	Pre Median	Pre Average	Post Brightness	Post Median	Post Average	Net Pixels	Net Brightness	Net Median	Area Sq cm	VITAE Mass
D	R	1	0.037	16873	128049	6	7.589	130608	6	7.746	1816	18119	8	103.702	0.059
D	R	2	0.074	17091	129725	6	7.590	137848	6	8.070	1911	23065	10	105.055	0.136
D	R	3	30.058	16978	128271	6	7.555	486833	9	28.666	5786	389711	46	104.446	5.460
D	R	4	60.042	16304	124184	6	7.617	810551	14	49.523	7417	723893	85	100.658	9.936
D	R	5	90.026	15495	105007	6	6.777	990082	20	63.913	8913	928711	97	95.270	14.527
D	R	6	120.01	17292	130279	6	7.534	1270146	28	73.453	9738	1189879	124	106.347	17.595
D	L	1	0.037	16052	107840	6	6.718	110190	6	6.868	665	8741	9	98.665	0.059
D	L	2	0.074	15649	104708	6	6.691	122047	6	7.762	1888	25152	10	96.697	0.136
D	L	3	30.058	16624	109657	6	6.596	480504	10	28.899	6654	400316	41	102.257	5.460
D	L	4	60.042	14318	81659	5	5.700	671808	12	46.917	7751	629532	71	88.063	9.936
D	L	5	90.026	13738	75826	5	5.519	908614	35	66.129	9222	877718	91	84.502	14.527
D	L	6	120.01	13709	75198	5	5.485	1053023	51	76.823	9833	1026125	104	84.299	17.595

Table H.3. Simulated Exposures - Subject 16

Side	Hand		Actual Mass (ug)	Pixels	Pre Brightness	Pre Median	Pre Average	Post Brightness	Post Median	Post Average	Net Pixels	Net Brightness	Net Median	Area (sq cm)	VITAE Mass (ug)
P	R	1	0.073	21772	984276	47	45.208	982281	46	45.024	2191	101184	45	133.898	0.103
P	R	2	0.284	20329	934818	47	45.984	968179	49	47.240	2054	109258	54	125.023	0.153
P	R	3	2.555	20936	941233	47	44.958	1151102	55	54.809	7020	468369	64	128.756	1.098
P	R	4	6.347	21397	966562	47	45.173	1275811	58	59.219	8480	627400	68	131.592	1.910
P	R	5	19.359	21110	957576	47	45.361	1310570	58	62.177	8379	684072	69	129.827	3.006
P	R	6	31.879	21052	953524	47	45.293	1352113	55	64.182	7245	680235	82	129.470	4.788
P	R	7	43.908	20569	932155	47	45.318	1417278	57	68.623	7744	787340	86	126.499	6.864
P	R	8	58.393	19836	904549	47	45.601	1419587	57	71.577	7430	809130	93	121.991	8.173
P	R	10	168.373	21353	963991	47	45.145	1760635	58	82.134	8451	1130218	111	131.321	19.917
P	L	1	0.073	20758	893346	45	43.036	905958	45	43.631	1527	72421	51	127.662	0.088
P	L	2	0.318	18176	804981	46	44.288	8511620	48	46.552	2214	126321	58	111.782	0.206
P	L	3	2.393	21252	906673	45	42.663	1088197	52	51.301	7011	441568	61	130.700	0.938
P	L	4	6.873	20842	888717	45	42.641	1153641	53	55.137	8318	569002	64	128.178	1.505
P	L	5	36.086	20740	895107	45	43.158	1208265	53	58.291	7760	609121	66	127.551	2.637
P	L	6	57.935	20514	877077	45	42.755	1269419	52	61.856	7305	670869	80	126.161	4.384
P	L	7	72.419	20257	871174	45	43.006	1293908	52	63.814	7017	688602	88	124.581	5.442
P	L	8	78.557	19539	830894	45	42.525	1286592	52	65.908	6549	694857	96	120.165	6.446
P	L	10	170.862	20097	855305	45	42.559	1585660	54	79.050	8315	1048160	102	123.597	17.196

Table H.3. Continued

Side	Hand		Actual Mass (ug)	Pixels	Pre Brightness	Pre Median	Pre Average	Post Brightness	Post Median	Post Average	Net Pixels	Net Brightness	Net Median	Area (sq cm)	VITAE Mass (ug)
D	R	1	0.035	19601	504343	25	25.730	537252	27	27.426	2838	90593	31	120.546	0.107
D	R	2	0.07	18960	494926	26	26.104	535950	28	28.264	3608	116504	32	116.604	0.126
D	R	3	0.105	19733	511031	26	25.897	571811	28	28.973	4772	160975	33	121.358	0.190
D	R	4	0.14	20319	521085	25	25.645	600677	29	29.560	6242	210562	33	124.962	0.251
D	R	5	29.323	20436	530072	26	25.938	1474891	35	72.210	10033	1174163	73	125.681	22.978
D	R	6	58.506	21214	548040	26	25.833	1932773	37	91.298	11084	1638173	150	130.466	37.368
D	R	7	87.689	20902	540798	26	25.873	2244922	43	107.069	12203	1984430	190	128.547	47.928
D	R	8	116.872	21698	557372	26	25.288	2405408	46	110.833	12344	2131501	211	133.443	52.355
D	L	1	0.035	20037	461882	23	23.051	490113	24	24.465	1699	50196	27	123.228	0.065
D	L	2	0.07	19921	471499	23	23.668	521555	26	26.184	3081	101097	30	122.514	0.135
D	L	3	0.105	19700	464272	23	23.567	540936	27	27.475	4372	148469	32	121.155	0.207
D	L	4	0.14	20683	481975	23	23.303	582416	27	28.131	5773	192860	31	127.200	0.272
D	L	5	29.323	19657	452890	23	23.040	1353320	35	68.868	9897	1091541	72	120.891	18.532
D	L	6	58.506	19609	460961	23	23.508	1720532	37	87.746	9704	1456276	160	120.595	29.827
D	L	7	87.689	20345	471202	23	23.161	1902162	42	93.523	11584	1657115	141	125.122	34.210
D	L	8	116.872	19253	444522	23	23.088	2042240	47	106.068	11384	1829549	185	118.406	40.643

Table H.4. Simulated Exposures - Subject 17

Side	Hand		Actual Mass (ug)	Pixels	Pre Brightness	Pre Median	Pre Average	Post Brightness	Post Median	Post Average	Net Pixels	Net Brightness	Net Median	Area cm^2	VITAE Mass (ug)
P	R	1	0.052	18879	944850	53	50.048	957535	53	50.709	1074	58388	55	116.11	0.088
P	R	2	0.243	19353	967274	53	49.981	981256	53	50.732	1034	55469	55	119.02	0.081
P	R	4	2.712	19800	968674	52	48.923	1039903	54	52.528	2432	158190	68	121.77	0.089
P	R	5	17.693	20069	991453	52	49.402	1107598	54	55.195	3761	286274	75	123.42	1.475
P	R	6	28.36	19113	958707	53	50.160	1119231	56	58.559	4246	362218	81	117.54	2.243
P	R	7	28.958	19227	958664	53	49.860	1179757	57	61.363	5098	458272	84	118.25	3.066
P	R	8	27.639	20080	990861	52	49.346	1278617	58	63.689	6022	561549	88	123.49	7.085
P	R	9	93.917	19265	956094	52	49.630	1373734	58	71.326	5813	680841	106	118.48	12.939
P	R	10	157.319	19194	958223	52	49.923	1542370	60	80.374	7175	921040	115	118.04	19.917
P	L	1	0.052	18754	860366	49	45.876	915891	51	48.511	2217	130572	59	115.34	0.228
P	L	2	0.398	18221	838260	49	46.005	875422	50	48.050	1294	70419	56	112.06	0.110
P	L	3	2.458	17896	823708	49	46.027	848843	49	47.435	1665	82912	47	110.06	0.119
P	L	4	5.981	17420	796852	49	46.221	854600	51	49.582	2910	178782	63	107.13	0.351
P	L	5	42.678	17817	828764	50	46.515	959561	51	53.866	4114	316265	73	109.57	1.104
P	L	6	72.086	17820	826237	49	46.366	1040786	54	58.396	5623	460016	76	109.59	1.192
P	L	7	94.205	17332	808432	50	46.644	1079411	56	62.293	6146	539317	80	106.59	2.872
P	L	8	108.063	18030	818288	49	45.385	1167564	55	64.760	6495	620298	86	110.88	4.243
P	L	9	174.403	17793	818091	49	45.978	1297813	57	72.927	7369	792960	93	109.43	7.849
P	L	10	214.988	17168	799981	50	46.597	1410799	59	82.133	8120	971541	110	105.58	11.774

Table H.4. Continued

Side	Hand		Actual Mass (ug)	Pixels	Pre Brightness	Pre Median	Pre Average	Post Brightness	Post Median	Post Average	Net Pixels	Net Brightness	Net Median	Area cm^2	VITAE Mass (ug)
D	R	1	0.036	19752	449740	21	22.769	469567	22	23.807	1332	45597	31	121.47	0.094
D	R	2	0.072	19742	445332	21	22.559	491677	23	24.879	2133	78933	33	121.41	0.156
D	R	3	0.108	19436	444263	21	22.858	479515	22	24.670	1602	63101	33	119.53	0.144
D	R	4	0.144	20410	460236	21	22.550	520650	23	25.461	2833	102238	32	125.52	0.217
D	R	5	29.268	20020	445455	21	22.250	1341050	30	66.996	7676	1039608	121	123.12	20.777
D	R	6	58.392	20375	448925	21	22.033	1977208	46	97.146	11150	1746234	168	125.31	38.513
D	R	7	87.516	20838	467046	21	22.413	2326395	60	111.706	11919	2098417	205	128.15	49.826
D	R	8	116.64	20652	453198	21	21.945	2628151	92	127.260	13169	2436138	227	127.01	60.219
D	L	1	0.036	17280	359935	21	20.830	367264	20	21.252	3165	73026	17	106.27	0.096
D	L	2	0.072	16723	350572	21	20.963	374035	21	22.360	1733	57834	32	102.85	0.098
D	L	3	0.108	16986	356329	21	20.978	372946	21	21.956	21114	61236	30	104.46	0.091
D	L	4	0.144	18305	397322	21	21.706	429405	22	23.425	1784	62420	32	112.58	0.120
D	L	5	29.268	18991	406382	21	21.399	1214349	29	63.916	7931	955758	96	116.79	17.682
D	L	6	58.392	19569	420301	21	21.478	1955220	48	99.904	10924	1748538	177	120.35	38.487
D	L	7	87.516	19495	417664	21	21.424	2326125	81	119.368	12194	2151258	215	119.89	49.773
D	L	8	116.64	18774	406568	21	21.656	2581126	149	137.491	13178	2440833	228	115.46	57.357

Table H.5. Simulated Exposures - Subject 18

Side	Hand		Actual Mass (ug)	Pixels	Pre Brightness	Pre Median	Pre Average	Post Brightness	Post Median	Post Average	Net Pixels	Net Brightness	Net Median	Area cm^2	VITAE Mass (ug)
P	R	1	0.073	14443	655863	47	45.410	622377	45	43.122	2104	81645	42	88.82	0.075
P	R	2	0.369	14621	660086	47	45.146	654779	46	44.811	1863	84582	44	89.92	0.115
P	R	3	2.021	15090	682576	47	45.234	747355	48	49.517	3228	215979	68	92.80	0.595
P	R	4	7.167	14443	645072	47	44.663	766367	49	53.054	4015	314178	76	88.82	1.274
P	R	5	20.919	15429	688392	47	44.617	935917	50	60.667	4871	471310	91	94.89	3.112
P	R	6	28.593	15225	672598	47	44.177	1007798	52	66.202	5161	555771	102	93.63	4.880
P	R	7	39.99	14181	632117	47	44.575	1039636	55	73.056	5753	656081	106	87.21	6.916
P	R	8	44.408	14519	653948	47	45.041	1115310	57	76.812	6429	749089	109	89.29	8.490
P	R	9	86.041	15336	683901	47	44.594	1320364	57	86.084	6660	927778	129	94.32	16.352
P	R	10	120.697	14670	651076	47	44.381	1399288	59	95.384	7042	1048014	139	90.22	21.685
P	L	1	0.073	15290	612844	42	40.081	647710	44	42.097	1774	91177	52	94.03	0.144
P	L	2	0.355	15329	614769	42	40.105	677496	46	44.269	3112	170777	54	94.27	0.295
P	L	3	1.867	14799	602626	43	40.721	690055	46	46.625	4158	246767	58	91.01	0.514
P	L	4	5.88	14586	590628	43	40.493	721181	48	49.535	4682	308831	63	89.70	0.825
P	L	5	23.324	14810	582760	43	39.349	817261	50	55.194	5603	432833	72	91.08	1.807
P	L	6	36.65	15083	599579	43	39.752	896716	50	59.602	5945	514952	78	92.76	3.115
P	L	7	40.069	14441	577166	43	39.967	937644	52	64.934	6231	590550	85	88.81	4.557
P	L	8	38.44	14124	581748	43	41.119	1005562	54	71.175	6908	686945	89	86.86	5.896
P	L	9	75.421	13538	559523	43	41.330	1127124	57	83.250	7055	846823	107	83.26	11.331
P	L	10	97.982	14032	578892	43	41.255	1271975	59	90.700	7854	1000921	112	86.30	16.105

Table H.5. Continued

Side	Hand		Actual Mass (ug)	Pixels	Pre Brightness	Pre Median	Pre Average	Post Brightness	Post Median	Post Average	Net Pixels	Net Brightness	Net Median	Area cm^2	VITAE Mass (ug)
D	R	1	0.034	14051	412001	28	29.321	385300	26	27.429	3066	69822	22	86.41	0.045
D	R	2	0.068	13888	406169	28	29.246	393937	26	28.341	2452	62274	23	85.41	0.053
D	R	3	0.102	14571	421300	28	28.914	429377	28	29.494	1739	62093	41	89.61	0.094
D	R	4	14.912	14547	429936	28	29.555	850066	35	58.456	5043	553979	106	89.46	6.562
D	R	5	29.722	14941	434372	28	29.072	1131453	42	75.916	6856	880564	121	91.89	14.054
D	R	6	44.53	15045	438021	28	29.114	1405765	52	93.233	8170	1186153	144	92.53	22.791
D	R	7	75.845	14420	423179	28	29.347	1525703	63	106.165	8276	1333523	168	88.68	29.741
D	R	8	107.158	14560	428070	28	29.400	1612156	67	110.695	8595	1422263	179	89.54	32.683
D	L	1	0.034	15270	391307	25	25.626	388674	24	25.478	1960	46754	21	93.91	0.047
D	L	2	0.068	13852	369282	26	26.659	381681	26	27.554	1486	43611	26	85.19	0.054
D	L	3	0.102	14929	379666	25	25.431	425166	27	28.479	2889	94616	29	91.81	0.133
D	L	4	14.912	15438	392441	25	25.420	819409	34	53.071	6125	552469	79	94.94	5.652
D	L	5	29.722	15523	387120	25	24.938	1148822	42	73.936	7947	929346	108	95.47	13.439
D	L	6	44.53	16019	398486	25	24.876	1436917	53	89.712	9035	1229568	126	98.52	22.178
D	L	7	75.845	15446	392704	25	25.424	1626652	62	104.918	9047	1432592	160	94.99	30.612
D	L	8	107.158	15880	404140	25	25.450	1803182	69	113.551	9609	1616853	189	97.66	36.803